THE JOURNAL OF BIOLOGICAL CHEMISTRY VOL. 290, NO. 5, pp. 2670–2688, January 30, 2015

The TRPM8 Protein Is a Testosterone Receptor

*II. FUNCTIONAL EVIDENCE FOR AN IONOTROPIC EFFECT OF TESTOSTERONE ON TRPM8**

Received for publication, September 12, 2014, and in revised form, November 27, 2014 Published, JBC Papers in Press, December 5, 2014, DOI 10.1074/jbc.M114.610873

Swapna Asuthkar[‡1], Lusine Demirkhanyan[‡1], Xiaohui Sun[‡], Pia A. Elustondo[§], Vivek Krishnan[¶], Padmamalini Baskaran[¶], Kiran Kumar Velpula[‡], Baskaran Thyagarajan[¶], Evgeny V. Pavlov[§‖], and Eleonora Zakharian[‡2]

From the [‡]Department of Cancer Biology and Pharmacology, University of Illinois College of Medicine, Peoria, Illinois 61605, [§]Dalhousie University, Halifax, Nova Scotia B3H 4R2, Canada, the [¶]College of Health Sciences, School of Pharmacy, University of Wyoming, Laramie, Wyoming 82071, and the [‖]Department of Basic Sciences, College of Dentistry, New York University, New York, New York 10010

Background: TRPM8 channels are highly expressed in prostate tissues, where the role of this cold receptor is not well understood.
Results: Testosterone activates TRPM8 in various cellular systems and in the planar lipid bilayers.
Conclusion: TRPM8 is an ionotropic testosterone receptor.
Significance: TRPM8 channels may be implicated in various physiological processes regulated by androgens.

Testosterone is a key steroid hormone in the development of male reproductive tissues and the regulation of the central nervous system. The rapid signaling mechanism induced by testosterone affects numerous behavioral traits, including sexual drive, aggressiveness, and fear conditioning. However, the currently identified testosterone receptor(s) is not believed to underlie the fast signaling, suggesting an orphan pathway. Here we report that an ion channel from the transient receptor potential family, TRPM8, commonly known as the cold and menthol receptor is the major component of testosterone-induced rapid actions. Using cultured and primary cell lines along with the purified TRPM8 protein, we demonstrate that testosterone directly activates TRPM8 channel at low picomolar range. Specifically, testosterone induced TRPM8 responses in primary human prostate cells, PC3 prostate cancer cells, dorsal root ganglion neurons, and hippocampal neurons. Picomolar concentrations of testosterone resulted in full openings of the purified TRPM8 channel in planar lipid bilayers. Furthermore, acute applications of testosterone on human skin elicited a cooling sensation. Our data conclusively demonstrate that testosterone is an endogenous and highly potent agonist of TRPM8, suggesting a role of TRPM8 channels well beyond their well established function in somatosensory neurons. This discovery may further imply TRPM8 channel function in testosterone-dependent behavioral traits.

Testosterone is a steroid hormone from the androgen group that is widely known for its classic genomic actions and its regulatory role in growth and development. The genomic actions of androgens are mediated by the androgen receptor (AR)[3] protein, a member of the nuclear receptor family of transcription factors (1, 2). The steroid-AR complex is translocated to the nucleus, where it binds to promoters and stimulates gene expression (3). At the same time, it has long been recognized that testosterone exerts rapid non-genomic actions (4), which, in particular, may stimulate rapid Ca^{2+} influxes (5). However, to date, the molecular targets and mechanisms of non-genomic testosterone-induced events remained as an orphan pathway.

In our efforts to pinpoint the non-genomic targets of testosterone, we discovered the key involvement of an ion channel protein from the transient receptor potential (TRP) superfamily of the melastatin group, TRPM8. The TRPM8 protein is expressed in various tissues, including the brain, sensory neurons, lungs, heart, and, notably, the prostate (6, 7). Although the role of TRPM8 as the cold and menthol receptor has been well established in the peripheral nervous system (8–10), its role in other tissues is not well understood because no endogenous agonists of TRPM8 have been identified thus far. In the accompanying paper (19), immunohistochemistry and co-immunoprecipitation experiments with human tissues and cultured cells revealed that endogenous testosterone directly interacts with TRPM8. In the present study, we demonstrate that testosterone directly activates TRPM8 in different cellular systems. Specifically, testosterone-induced TRPM8 responses were detected in prostate cancer cells (PC3), dorsal root ganglion (DRG) neurons, hippocampal neurons, and human embryonic kidney (HEK-293) cells. In addition, testosterone exerted its agonist action on purified TRPM8 channels incorporated into planar lipid bilayers. The addition of testosterone in picomolar concentrations resulted in the full opening of TRPM8. Using a

* This work was supported, in whole or in part, by National Institutes of Health Grant R01GM098052 (to E. Z.). This work was also supported by Grant G-13-00030008 from the Heart and Stroke Foundation of Canada (to E. P.).
[1] Both authors contributed equally to this work.
[2] To whom correspondence should be addressed: Dept. of Cancer Biology and Pharmacology, University of Illinois, College of Medicine, 1 Illini Dr., Peoria, IL 61605. Tel.: 309-680-8621; Fax: 309-671-3442; E-mail: zakharel@uic.edu.

[3] The abbreviations used are: AR, androgen receptor; DiC_8, diacylglycerol C8; 5S-G, S819G/S820G/S823G/S824G/S827G; M8-B, *N*-(2-aminoethyl)-*N*-(4-(benzyloxy)-3-methoxybenzyl)thiophene-2-carboxamide hydrochloride; DRG, dorsal root ganglion; POPC, 1-palmitoyl-2-oleoyl-glycero-3-phosphocoline; POPE, 1-palmitoyl-2-oleoyl-glycero-3-phosphoethanolamine; PIP_2, phosphatidylinositol 4,5-bisphosphate; pS, picosiemens; PHB, polyhydroxybutyrate.

membrane-impermeable analog of testosterone in combination with mutagenesis, we identified residues located on the extracellular side of TRPM8 that contribute to the formation of the testosterone-binding site. The potential physiological relevance of testosterone-TRPM8 interactions was indicated in the experiments with human volunteers, who experienced a cold sensation in response to acute testosterone applications to the skin.

Overall, our data revealed a novel role of the TRPM8 channel as a testosterone receptor. This discovery suggests a central role of TRPM8 in important biological processes, including reproductive functions and the regulation of the central nervous system.

EXPERIMENTAL PROCEDURES

Cell Culture—HEK-293 cells were maintained in minimal essential medium solution (Invitrogen) supplemented with 10% fetal bovine serum (Invitrogen) and 1% penicillin/streptomycin. The cells were transfected with the rat TRPM8 cDNA using the Effectene reagent (Qiagen, Chatsworth, CA). The TRPM8 stable cell line was developed with TRPM8 tagged with Myc on the N terminus, as described previously (11).

Rat embryonic dorsal root ganglion (DRG) neurons and rat hippocampal neurons were purchased from Lonza (Allendale, NJ) and cultured in primary neuron basal medium. The fully supplemented medium contained 2 mM L-glutamine, 50 μg/ml gentamicin, 37 μg/ml amphotericin, and 2% NSF-1. For the inhibition of Schwann cells and glial cells, mitotic inhibitors were added to the medium (uridine (17.5 μg/ml) and 5-fluoro-2-deoxyuridine (7.5 μg/ml)). The neurons were cultured for 3–4 days before the transfection.

DRG neurons or hippocampal neurons were transfected with TRPM8 cDNA with the Nucleofector^{TM} kit (Lonza), following the instructions from the manufacturer. Briefly, laminin-coated coverslips were preincubated with 300 μl of the medium at 37 °C. Cells were centrifuged at 80 × *g* for 5 min at room temperature, and the pellet was carefully resuspended in Nucleofector solution (100 μl/sample) with the subsequent addition of DNA. The cell/DNA suspension was then transferred into the cuvette and treated in the Nucleofector with program G-013. After the addition of 500 μl of the pre-equilibrated culture medium to the cuvette, the neurons were gently transferred to the prepared culture dish with the coated coverslip. Then DRG neurons were cultured for 24–48 h.

The prostate cancer cell lines LNCaP, PC-3, and RWPE2, were obtained from the American Type Culture Collection (Manassas, VA) and cultured as directed. LNCaP cells were cultured in RPMI medium supplemented with 2 mM L-glutamine, 1.5 g/liter sodium bicarbonate, 4.5 g/liter glucose, 10 mM HEPES, and 1.0 mM sodium pyruvate (Invitrogen). PC3 cells were cultured in Dulbecco's modified Eagle's medium (DMEM)/F12K (1:1). Both media contained 10% fetal bovine serum (Invitrogen) and 5% penicillin/streptomycin. RWPE-2 cells are cultured in keratinocyte serum-free medium supplemented with 0.05 mg/ml bovine pituitary extract and 5 ng/ml epidermal growth factor. All of the cells were maintained in a 37 °C incubator in a 5% CO_2 humidified atmosphere.

Intracellular Ca^{2+} Measurements—The extracellular solution used in ratiometric $[Ca^{2+}]_i$ measurements contained 137 mM NaCl, 5 mM KCl, 1.8 mM $CaCl_2$, 1 mM $MgCl_2$, 10 mM glucose, and 10 mM Hepes, pH 7.4. Cells were incubated with 2 μM Fura-2 acetoxymethyl ester (Tef Labs, Austin, TX) for 30 min at room temperature. The fluorescence signals of the cells grown on the coverslips were measured using alternating excitation at 340 and 380 nm, and emission was detected at 510 nm. The ratio of fluorescence (340 nm/380 nm) was plotted against time. The obtained values of ratios from each coverslips were first analyzed, and then the mean values of stimuli-induced signals were combined, and statistically averaged values with mean errors were plotted in the summary graphs. The total number of measurements/coverslips (*n*) are indicated in the figure legends. The measurements were performed using a Photon Technology International (Birmingham, NJ) imaging system mounted on an Zeiss-AXIO observed D1 microscope, equipped with a DeltaRAM excitation light source or with a Ratiomaster 5 imaging system (Photon Technology International) equipped with a Cool-snap HQ2 (Roper) camera.

Preparation of the TRPM8 Protein from Human Embryonic Kidney Cells—HEK-293 cells stably expressing TRPM8 were grown to 70–80% confluence, washed, and collected with PBS. Cells were harvested and resuspended in NCB buffer, containing 500 mM NaCl, 50 mM NaH_2PO_4, 20 mM Hepes, 10% glycerol, pH 7.5, with the addition of 1 mM of protease inhibitor PMSF, 5 mM β-mercaptoethanol. Then the cells were lysed by the freeze-thawing method and centrifuged at low speed to remove cell debris and DNA. The supernatant was further centrifuged at 40,000 × *g* for 2.5 h, and the pellet was resuspended in NCB buffer with the addition of a protease inhibitor mixture (Roche Applied Science), 0.1% Nonidet P-40 (Roche Applied Science), and 0.5% dodecylmaltoside (Calbiochem). The suspension was incubated overnight at 4 °C on a shaker with gentle agitation and then centrifuged for 1 h at 40,000 × *g*. Further, the TRPM8 protein was purified by immunoprecipitation with anti-Myc-IgG conjugated to A/G protein magnetic beads (Pierce, Thermo Scientific), following the procedure provided by the manufacturer. All steps of the purification were performed at 4 °C. For the planar lipid bilayer experiments, the protein was eluted with Myc-peptide (50 μg/ml).

Purification of AR—Immunoprecipitation of AR protein was carried out by incubating 400 μg of cell extracts obtained from HEK-293 cells with AR-specific monoclonal antibody (1 μg) (Santa Cruz Biotechnology, Inc.) overnight at 4 °C on an end-to-end rotator. Next, the Catch and Release version 2.0 IP kit (Millipore, Temecula, CA) was used to immunoprecipitate and elute proteins in non-denaturing buffers according to the manufacturer's instructions.

Planar Lipid Bilayer Measurements—Planar lipid bilayer measurements were performed as described previously (11, 13, 14). Planar lipid bilayers were formed from a solution of synthetic 1-palmitoyl-2-oleoyl-glycero-3-phosphocoline (POPC) and 1-palmitoyl-2-oleoyl-glycero-3-phosphoethanolamine (POPE; Avanti Polar Lipids, Birmingham, AL) in a 3:1 ratio in *n*-decane (Sigma-Aldrich). The solution was used to paint a bilayer in an aperture of ~150-μm diameter in a Delrin cup (Warner Instruments, Hamden, CT) between symmetric aqueous bathing

solutions of 150 mM KCl, 0.2 mM $MgCl_2$, 1 μM $CaCl_2$, 20 mM Hepes, pH 7.4, at 22 °C. All lipid bilayer experiments were performed in the presence of phosphatidylinositol 4,5-bisphosphate (PIP_2), unless specifically omitted as indicated. 2.5 μM DiC_8-PIP_2 (Cayman Chemical Comp.) dissolved in water was added to both compartments. All salts were ultrapure (>99%) (Sigma-Aldrich). Bilayer capacitances were in the range of 50–75 picofarads. After the bilayers had been formed, the TRPM8 protein from the micellar suspension (20 ng/ml) was added by painting. Unitary currents were recorded with an integrating patch clamp amplifier (Axopatch 200B, Axon Instruments). The trans solution (voltage command side) was connected to the CV 201A head stage input, and the cis solution was held at virtual ground via a pair of matched Ag-AgCl electrodes. Currents through the voltage-clamped bilayers (background conductance <1 pS) were filtered at the amplifier output (low pass, −3 decibels at 10 kHz, 8-pole Bessel response). Data were secondarily filtered at 100 Hz through an 8-pole Bessel filter (950 TAF, Frequency Devices) and digitized at 1 kHz using an analog-to-digital converter (Digidata 1322A, Axon Instruments), controlled by pClamp version 10.3 software (Axon Instruments). Single-channel conductance events, all points histograms, open probability, and other parameters were identified and analyzed using the Clampfit version 10.3 software (Axon Instruments).

Immunoblotting and Immunoprecipitation Assay—Immunoblotting and immunoprecipitation assays were done essentially as described in the accompanying paper (19).

Immunocytochemistry—DRG and hippocampal neurons transiently expressing Myc-TRPM8 or hippocampal neurons endogenously expressing TRPM8 were grown on 25-mm round glass coverslips and fixed with 2 ml of 4% paraformaldehyde in PBS at room temperature for 30 min. The cells were washed three times with PBS (2 ml) and treated with 2 ml of 100 mM glycine in PBS for 30 min. After washing with PBS twice, the cells were permeabilized with 300 μl of cold methanol at −20 °C for 5 min or with 0.1% Triton X-100 for 2 min at room temperature and then washed twice with 2 ml of PBS. The cells were then blocked with 3% BSA (for anti-Myc-IgG and anti-TRPM8-IgG) for 1 h at room temperature, followed by incubation with anti-Myc (Sigma-Aldrich) (1:2500) or anti-TRPM8 (Phoenix Pharmaceuticals, Inc.) (1:2000) antibodies in 3% BSA plus PBS overnight at room temperature. The next day, the cells were washed with PBS three times and then treated with Alexa secondary antibodies (1:3000) (Invitrogen) for another 1 h at room temperature. The cells were then washed three times with 2 ml of PBS, washed once with distilled water, and mounted on a glass slide with Immu-Mount (Pierce, Thermo Scientific) mounting medium. For immunocytochemical analysis, cells were observed with an Olympus BX61 confocal microscope (Minneapolis, MN) (×60 objective).

The immunocytochemistry experiments presented in Fig. 10*c* were done under non-permeabilized conditions. The experiments were performed on the WT TRPM8 and the TRPM8 mutants deficient in binding homopolymer polyhydroxybutyrate (PHB) that covalently modifies TRPM8 on the extracellular side of the channel (15). The HEK-293 cells were transfected with 1 μg of target DNA of the WT TRPM8 and the PHB-deficient mutants, S819G/S820G/S823G/S824G/S827G (5S-G) and Y826G. The cells were washed three times with PBS and fixed with 2% paraformaldehyde in PBS at room temperature for 30 min, washed twice with PBS, and incubated with 100 mM glycine for 30 min. Further, non-permeabilized cells were washed three times with PBS, blocked with 3% BSA in PBS for 1 h, and treated with 1 nM testosterone for 1 h at room temperature. Further, the cells were washed three times with PBS and incubated overnight with primary antibodies: mouse anti-Myc-IgG (1:2500) and sheep anti-DHT/testosterone-IgG (1:2000). Then cells were washed three times with PBS and incubated with the secondary antibodies (Alexa, Invitrogen). For the detection of Myc-tagged proteins, anti-mouse Alexa488 was used (1:3000). Alexa594-labeled anti-sheep antibody was used for testosterone visualization (1:3000). After 1 h of incubation with the secondary antibodies, cells were washed four times with PBS and mounted on a glass slide with Immu-Mount (Pierce, Thermo Scientific) mounting medium. Images were obtained by Olympus BX61 confocal microscope and were analyzed with ImageJ software.

Skin Test—Sixteen healthy human volunteers (eight female and eight male) between the ages of 18 and 55 years were recruited for the single-blinded test. Six microliters of testosterone dissolved in ethanol was applied in different concentrations and orders to the skin surface, alternating between the right and left arms, and the durations of the responses were recorded. The volunteers described their sensation and how long it lasted.

Statistical Analysis—Statistical analysis was performed using Origin version 9.0 software (Microcal Software Inc., Northampton, MA). Statistical significance was calculated using one-way analysis of variance followed by Fisher's least significant difference test, and data were expressed as mean ± S.E. In all figures, statistical significance is labeled the following way: *, $p < 0.05$; **, $p < 0.01$; ***, $p < 0.005$.

RESULTS

Testosterone Induces TRPM8 Activity in Various Cell Types—Direct binding of testosterone to TRPM8 (19) raised the question of what effect this steroid hormone exerts on channel function. To evaluate this interaction, we tested TRPM8 responses upon application of testosterone on various cell types, employing Ca^{2+}-imaging experiments (Figs. 1 and 2).

Prostate cancer PC3 cells with overexpressed TRPM8 channels showed strong testosterone-induced responses with highly transient kinetics and strong desensitization of the subsequent menthol-induced responses (Fig. 1*b*).

Next, we performed Ca^{2+}-imaging experiments on neurons cultured in serum-free medium. The DRG neurons with transiently expressed TRPM8 channels responded readily to testosterone applications in the picomolar range (Fig. 1*f*).

Similarly to DRG neurons, brain hippocampal neurons demonstrated stable testosterone-induced Ca^{2+} uptake (Fig. 2*b*). Furthermore, the testosterone-induced Ca^{2+} uptake was kinetically similar to the menthol-induced activation (Fig. 2, *a* and *b*). Both, endogenously and transiently expressing TRPM8, hippocampal neurons readily responded to testosterone beginning at femtomolar concentrations and reached a saturated Ca^{2+}

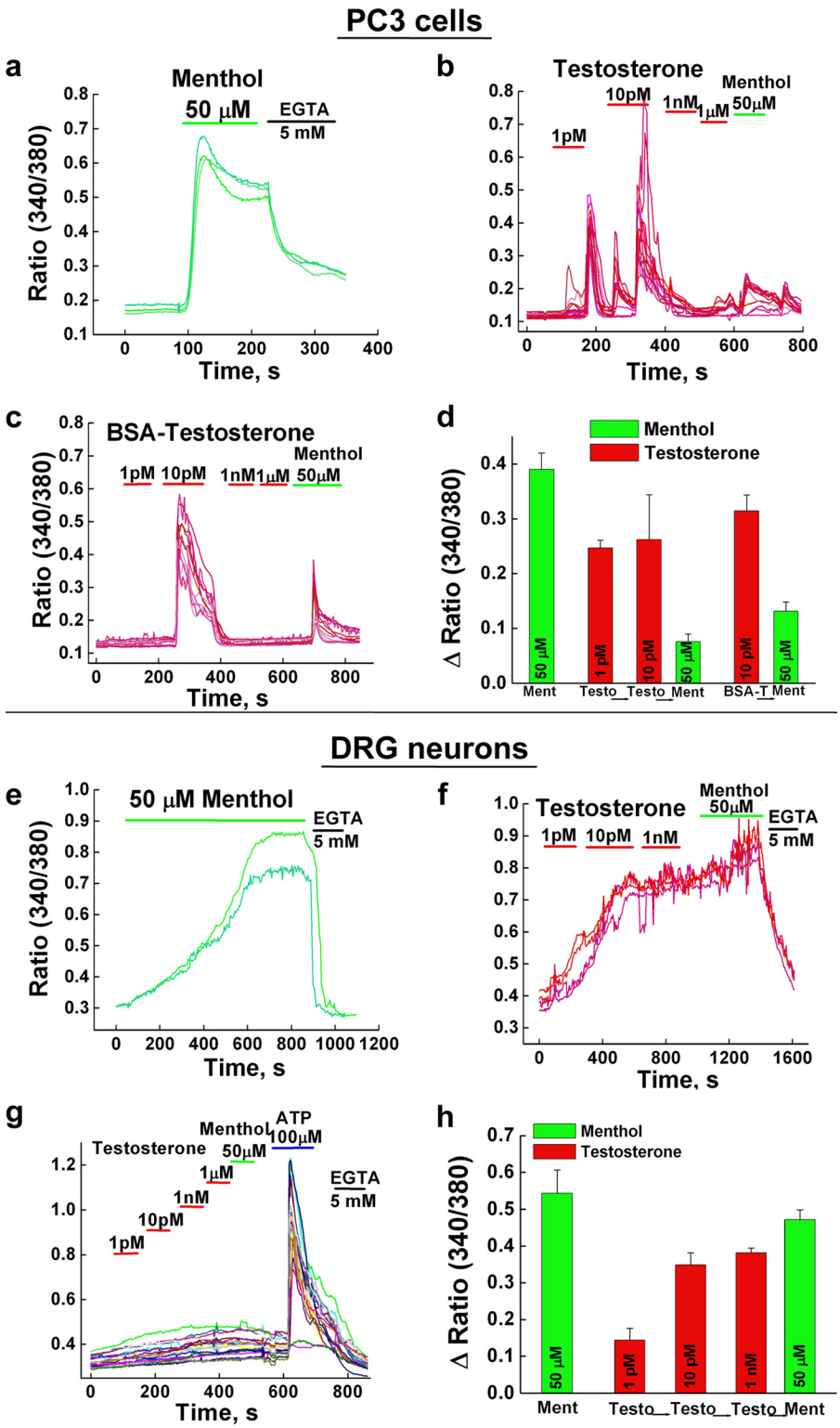

FIGURE 1. **Testosterone-induced TRPM8 activity in intracellular Ca^{2+} measurements in different cell types.** Fluorescence measurements of the intracellular Ca^{2+} concentration were performed on prostate PC3 cells and DRG neurons transiently expressing TRPM8. *a–d*, fluorescence measurements obtained from PC3 cells that were transiently transfected with the TRPM8 (0.7 μg) and GFP (0.2 μg) constructs. *a*, representative recording of the menthol-induced activation of TRPM8 channels ($n = 6$). *b*, representative recording of the testosterone-induced responses of TRPM8 channels ($n = 8$). *c*, TRPM8 channels were also induced by an impermeable variant of testosterone that was conjugated to BSA (*BSA-Testosterone*), indicating that at least one of the androgen-interacting sites is located on the extracellular side of the TRPM8 protein ($n = 6$). *d*, summary of the menthol- and testosterone-induced TRPM8 responses of PC3 cells (*error bars*, S.E.). *e–h*, fluorescence measurements obtained from DRG neurons transiently transfected with the TRPM8 (3 μg) and GFP (0.5 μg) constructs. *e*, representative recording of the menthol-induced activation of TRPM8 channels ($n = 4$). *f*, representative recording of the testosterone-induced responses of TRPM8 channels ($n = 6$). *g*, the control recording of DRG neurons that were not transfected with TRPM8 shows no response to either testosterone or menthol ($n = 3$). *h*, summary of the menthol- and testosterone-induced TRPM8 responses of DRG neurons (*error bars*, S.E.).

signal with a 1 pM concentration of the steroid (Fig. 2, *b*, *c*, *e*, and *g*). Menthol-irresponsive hippocampal neurons were also insensitive to testosterone applications (Fig. 2*f*). These results suggest that testosterone is a potent agonist of the TRPM8 channel.

Testosterone-induced TRPM8 Activity in HEK-293 Cells—Next, we tested testosterone-induced TRPM8 responses in the heterologous expression system, using HEK-293 cells. Unlike the neurons or prostate cells, testosterone applications on HEK-293 cells transiently or stably expressing TRPM8 elicited

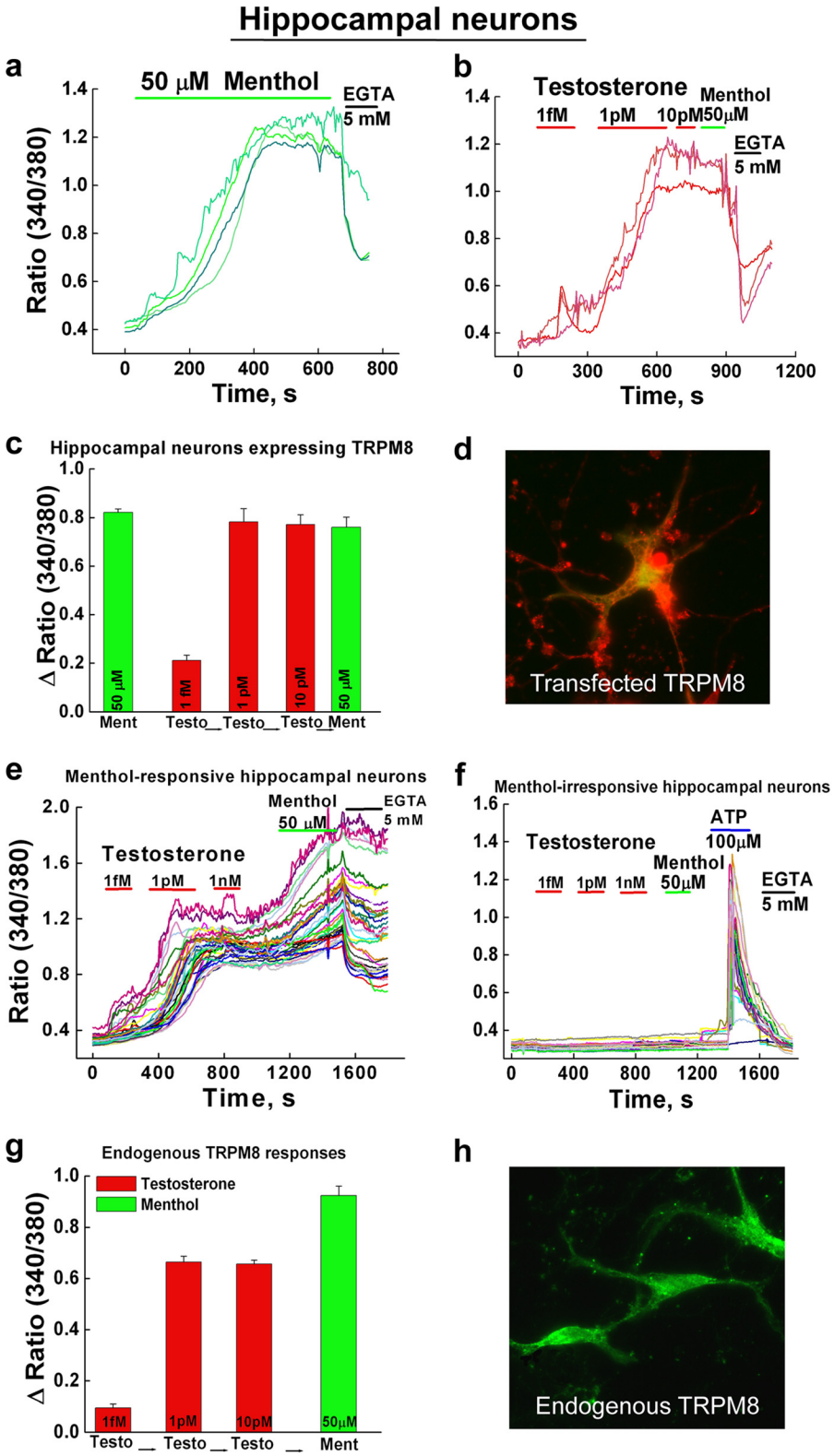

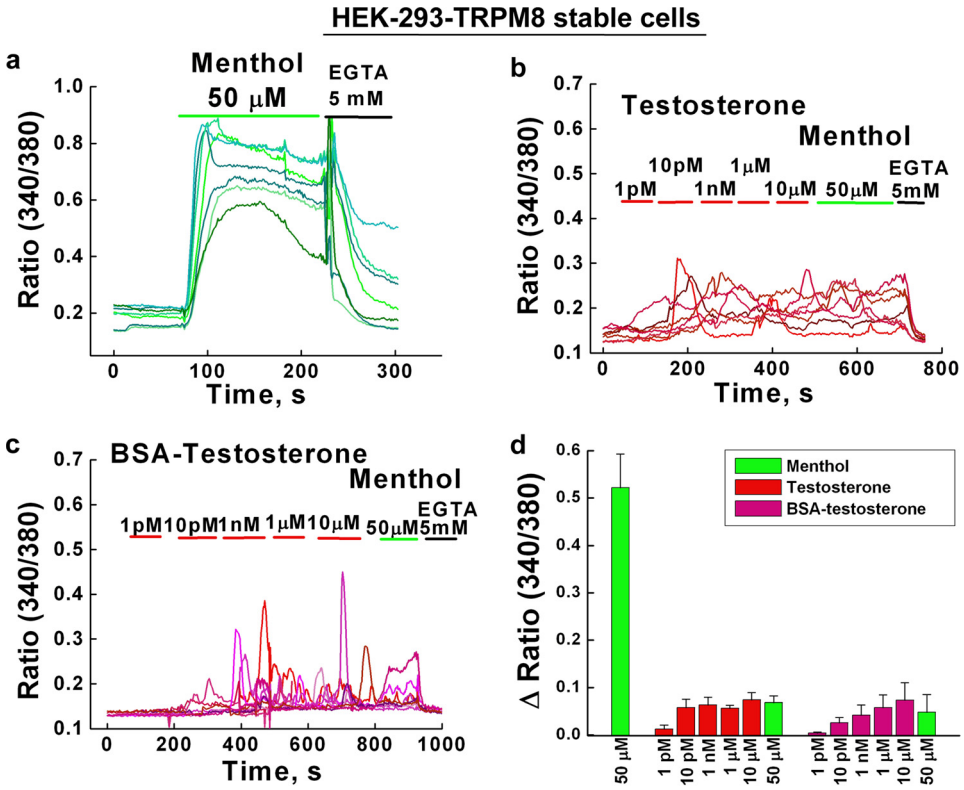

FIGURE 3. **Testosterone-induced Ca^{2+} signals observed on HEK-293 cells stably expressing TRPM8.** Fluorescence measurements of intracellular Ca^{2+} concentration were performed on HEK-293 cells expressing the TRPM8 protein. Shown are the menthol-induced Ca^{2+} response (*a*) and testosterone-induced (*b*) and impermeable analog BSA-testosterone-induced (*c*) TRPM8 activities. A summary is shown in *d*. *Error bars*, S.E.

low Ca^{2+} oscillations and further inhibited menthol-induced activation of TRPM8 (Fig. 3). This activity was dependent on the expression levels of the AR protein. Testosterone-induced TRPM8 responses in HEK-293 cells were of higher amplitude with co-expression of AR-siRNA (Fig. 4, *b* and *c*) or with application of the AR blocker hydroxyflutamide but still remained highly heterogeneous (Fig. 4, *f* and *g*). Interestingly, co-application of the AR inhibitor hydroxyflutamide (1 μM) significantly recovered menthol responses following testosterone applications (Fig. 4, *f*–*h*). Similar recovery of menthol-induced responses was observed with another AR inhibitor, cyproterone acetate (1 μM), and the 5α-reductase inhibitor finasteride (1 μM) (data not shown).

Variability of testosterone-induced Ca^{2+} responses in HEK-293 cells indicated unevenness of endogenous androgen levels and the possibility of the channel desensitization. Indeed, immunocytochemistry experiments showed the presence of endogenous testosterone in HEK-293 cells, where its pattern was highly colocalized with TRPM8 and also with AR (data not shown).

To address this issue, we cultured HEK-293 cells under the steroid-deprived conditions. Under these conditions, the fluorescence measurements of HEK-293 cells stably expressing TRPM8 channels demonstrated increased testosterone-induced responses after 18 h of deprivation, but the variability was still present among the cells (data not shown). After 38 h of the steroid deprivation, more homogeneous testosterone-induced TRPM8 responses were obtained, with both membrane-permeable and -impermeable testosterone analogs (Fig. 5).

To confirm that testosterone-induced activities are not due to nonspecific interactions, we tested TRPM8 responses upon applications of a similar lipophilic compound, using cholesterol. Cholesterol applications on HEK-293 cells stably or transiently expressing TRPM8 did not evoke any notable Ca^{2+} uptake and were followed by a strong activation with the subsequent menthol application (Fig. 6).

Together, these results favored the hypothesis that testosterone exerts an agonistic action on TRPM8. However, the testosterone-induced channel activity in this heterologous system

FIGURE 2. **Testosterone-induced TRPM8 activity in intracellular Ca^{2+} measurements in hippocampal neurons.** *a* and *b*, fluorescence measurements obtained from hippocampal neurons transiently transfected with TRPM8 (3 μg) and GFP (0.5 μg) constructs. *a*, representative recording of the menthol-induced activation of TRPM8 channels in hippocampal neurons ($n = 3$); *b*, representative recording of the testosterone-induced responses of TRPM8 channels in hippocampal neurons ($n = 8$). *c*, summary of the menthol- and testosterone-induced TRPM8 responses in hippocampal neurons (*error bars*, S.E.). *d*, immunocytochemistry image of the transiently expressed TRPM8 protein in hippocampal neurons, as detected with anti-Myc-IgG. The images were obtained with an Olympus-BX61 confocal microscope with a ×60 objective. Hippocampal neurons endogenously expressing TRPM8 channels respond to both testosterone and menthol. *e*, representative recording of the testosterone-induced and subsequent menthol-induced responses of TRPM8 channels in hippocampal neurons ($n = 5$). *f*, menthol-irresponsive hippocampal neurons are also insensitive to testosterone applications ($n = 3$). *g*, summary of the testosterone- and menthol-induced responses of endogenous TRPM8 channels in hippocampal neurons (*error bars*, S.E.). *h*, immunocytochemistry image of the endogenous TRPM8 protein in hippocampal neurons detected with anti-TRPM8-IgG. The images were obtained using an Olympus-BX61 confocal microscope with a ×60 objective.

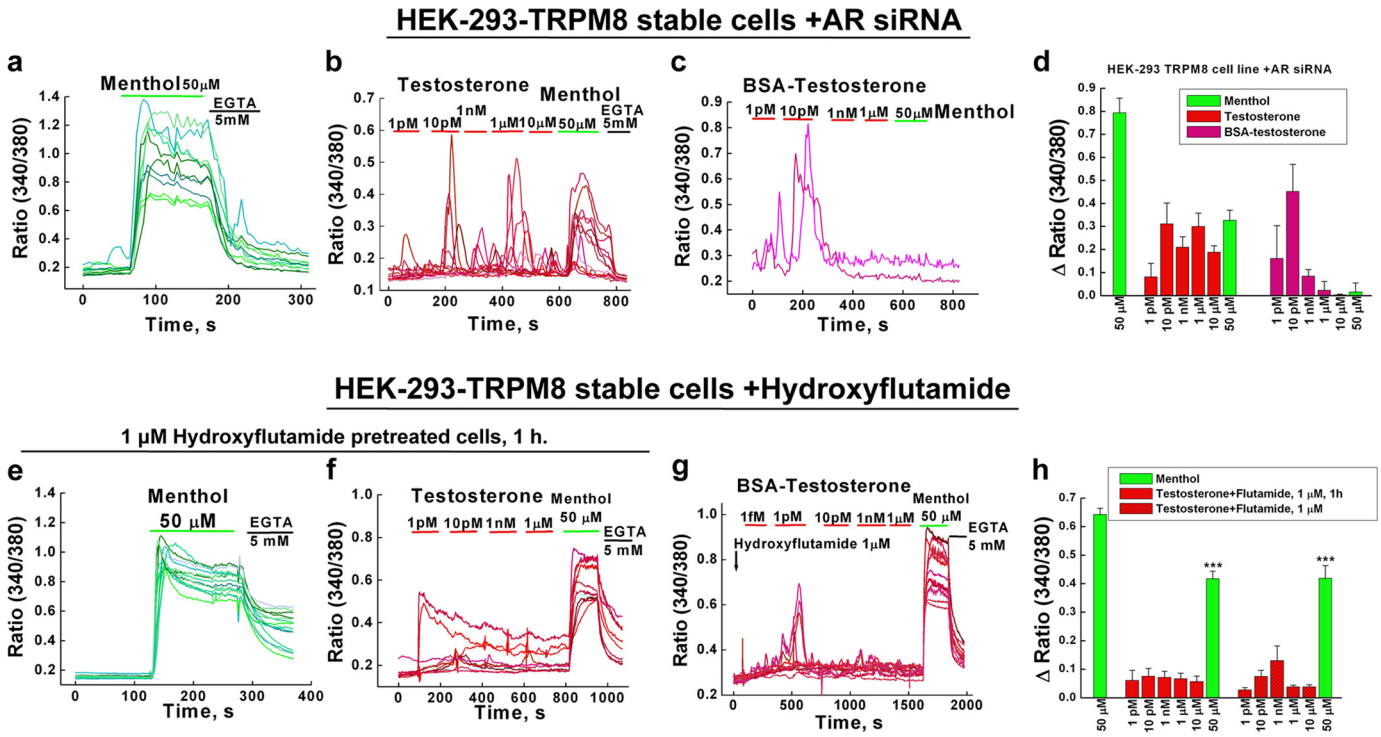

FIGURE 4. **The AR protein exerts inhibitory effects on TRPM8.** Fluorescence measurements of intracellular Ca^{2+} obtained from HEK-293-TRPM8 stable cells with co-expressed siRNA for the AR protein. TRPM8 activity was induced with menthol (*a*), testosterone (*b*), and BSA-testosterone (*c*) and showed heterogeneous responses of higher amplitude. A summary is shown in *d*. HEK-293-TRPM8 stable cells treated with AR inhibitor hydroxyflutamide show recovery of the subsequent menthol-induced responses. In *e* and *f*, cells were pretreated with 1 μM hydroxyflutamide for 1 h before application of the agonists. Shown are TRPM8 responses with menthol (*e*) and testosterone (*f*) applications. *g*, co-application of the AR inhibitor hydroxyflutamide (1 μM) with testosterone and menthol. A summary is shown in *h*. *Error bars*, S.E. ***, $p < 0.005$.

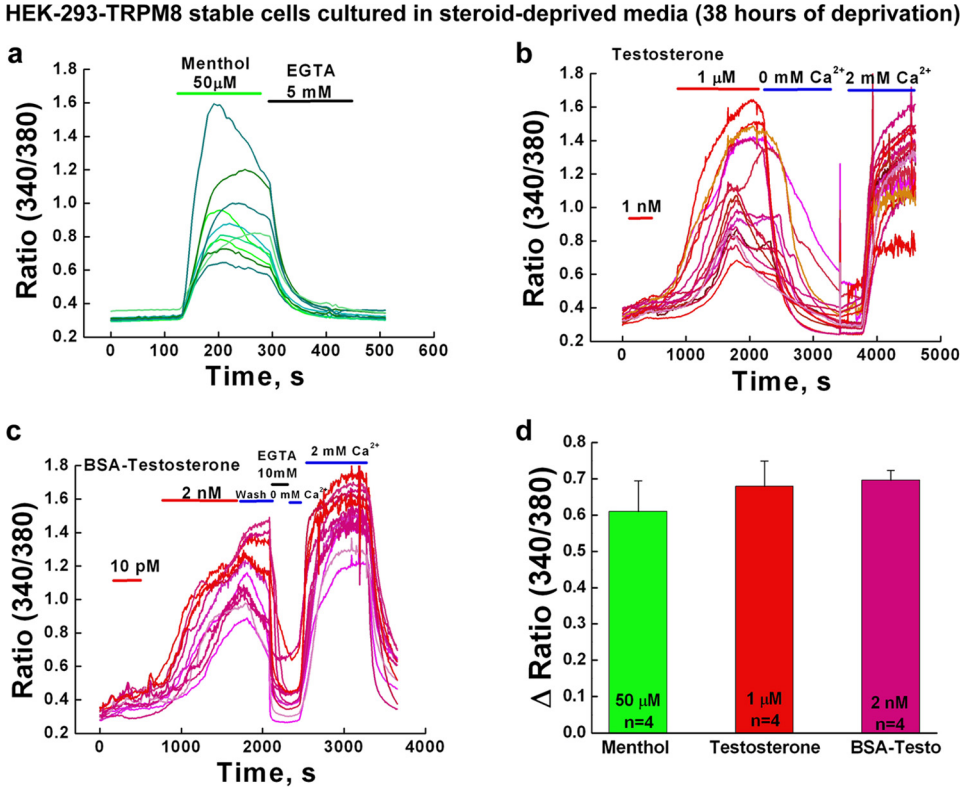

FIGURE 5. **Testosterone-induced Ca^{2+} uptake in HEK-293 TRPM8 stable cells cultured under the steroid-deprived conditions.** Fluorescence measurements of intracellular Ca^{2+} concentration were performed on HEK-293 cells stably expressing the TRPM8 protein. The cells were cultured in the steroid-deprived medium using 0.25% charcoal and 0.0025% dextran for up to 38 h. Menthol-induced (*a*), testosterone-induced (*b*), and BSA-testosterone-induced (c) TRPM8 activity is shown. A summary is presented in *d*. *Error bars*, S.E.

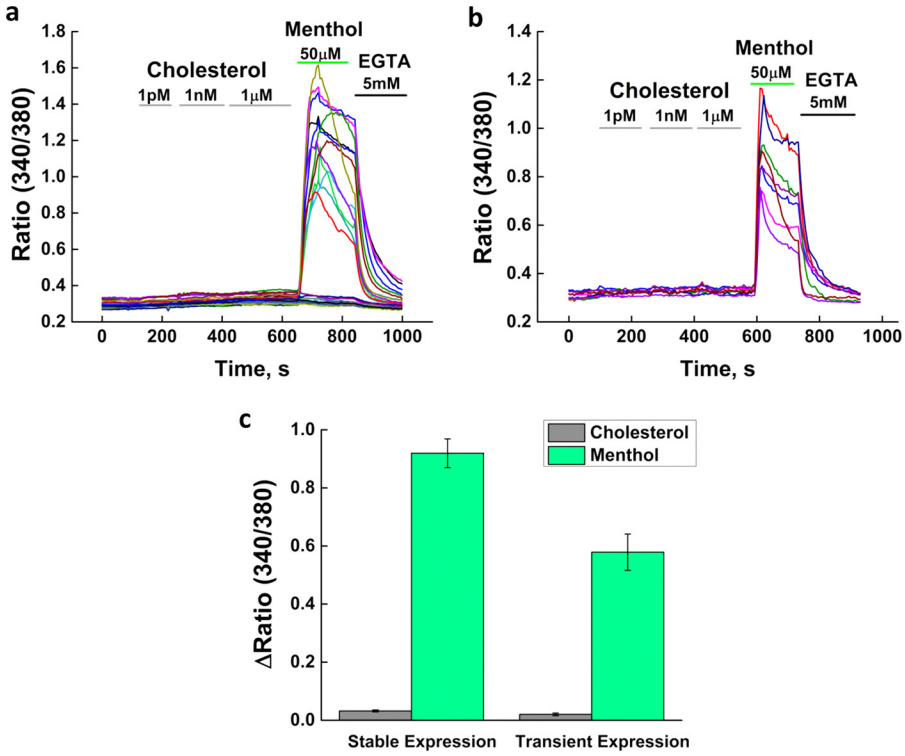

FIGURE 6. **Effect of cholesterol on TRPM8 channel activity.** Application of cholesterol (1 pM; 1 nM and 1 μM) does not induce Ca^{2+} uptake in HEK-293 cells stably (*a*; $n = 51$) or transiently expressing TRPM8 channel (*b*; $n = 16$). *c*, summary of the cholesterol- and menthol-induced responses of TRPM8. *Error bars*, S.E.

was complex and required further evaluation using a different approach.

Testosterone Directly Activates TRPM8 Channels in Planar Lipid Bilayers—Steroids are involved in regulating various cellular processes and metabolic pathways (16, 17). Therefore, it may be challenging to recognize direct channel activation based upon cellular responses, and more rigorous characterization is needed. To exclude the potential contributions from the complexity of various cellular pathways, we incorporated the purified TRPM8 protein into planar lipid bilayers to characterize testosterone-induced activity of the TRPM8 channel.

We found that testosterone readily activated TRPM8 in artificial lipid membranes. Moreover, the channel demonstrated highly organized gating transitions and stability (Fig. 7). In the planar lipid bilayers in the presence of PIP_2, TRPM8 was activated by testosterone added to both sides at picomolar solution concentrations, which is within the physiological range, and exhibited an EC_{50} of ~65 pM for activation with testosterone and ~21 nM with DHT (Fig. 7, *a* and *b*). The subsequent addition of the purified AR protein into the bilayer system (both sides) resulted in the complete inhibition of the channel, which may have resulted from the competitive androgen binding between the AR and TRPM8 proteins (Fig. 7*a*, *bottom traces*). The TRPM8 channel activated by testosterone demonstrated high stability (9–10 h) (*i.e.* the channels were open all day throughout the experiments).

Additionally, we tested specificity of the testosterone-evoked TRPM8 channel openings observed in the planar lipid bilayers by applying specific TRPM8 inhibitors. TRPM8 channels activated with testosterone were promptly inhibited with all tested TRPM8 antagonists (Fig. 7, *c* and *d*). It is noteworthy that TRPM8 inhibition with a novel TRPM8 antagonist, *N*-(2-aminoethyl)-*N*-(4-(benzyloxy)-3-methoxybenzyl)thiophene-2-carboxamide hydrochloride (M8-B) (18), occurred only upon its application onto one side of the channel, presumably extracellular, according to the inhibitory effects of this compound observed previously on intact cells (18). Unlike M8-B, application of polylysine was effective only when applied to the intracellular side of the channel, similar to previously demonstrated menthol-activated TRPM8 channels (11).

As a control, we tested what effect testosterone could exert on the planar lipid bilayers without protein. Even at high concentrations (up to 5 μM), testosterone did not affect the membrane stability, cause leak currents, or induce extra conductance (Fig. 7*e*).

We also performed mass spectrometric analysis on the TRPM8 protein obtained in the large scale purification assay. TRPM8 was purified by immunoprecipitation with Myc antibodies, as described previously (15). The liquid chromatography (LC) mass spectrometry (MS/MS) analysis demonstrated that TRPM8 presents the major protein fraction purified under these conditions, and among the other proteins present in the samples, there were no possible candidates of any other ion channels at the detectable level (Table 1).

Next, we compared testosterone-evoked TRPM8 activity with other agonists. Similarly to the icilin-induced channel activity (described previously (13)), the TRPM8 channel activated by testosterone demonstrated a linear current-voltage relationship (did not show current rectification specific to the menthol-evoked activation (11)) (Fig. 8, *a* and *b*) and also

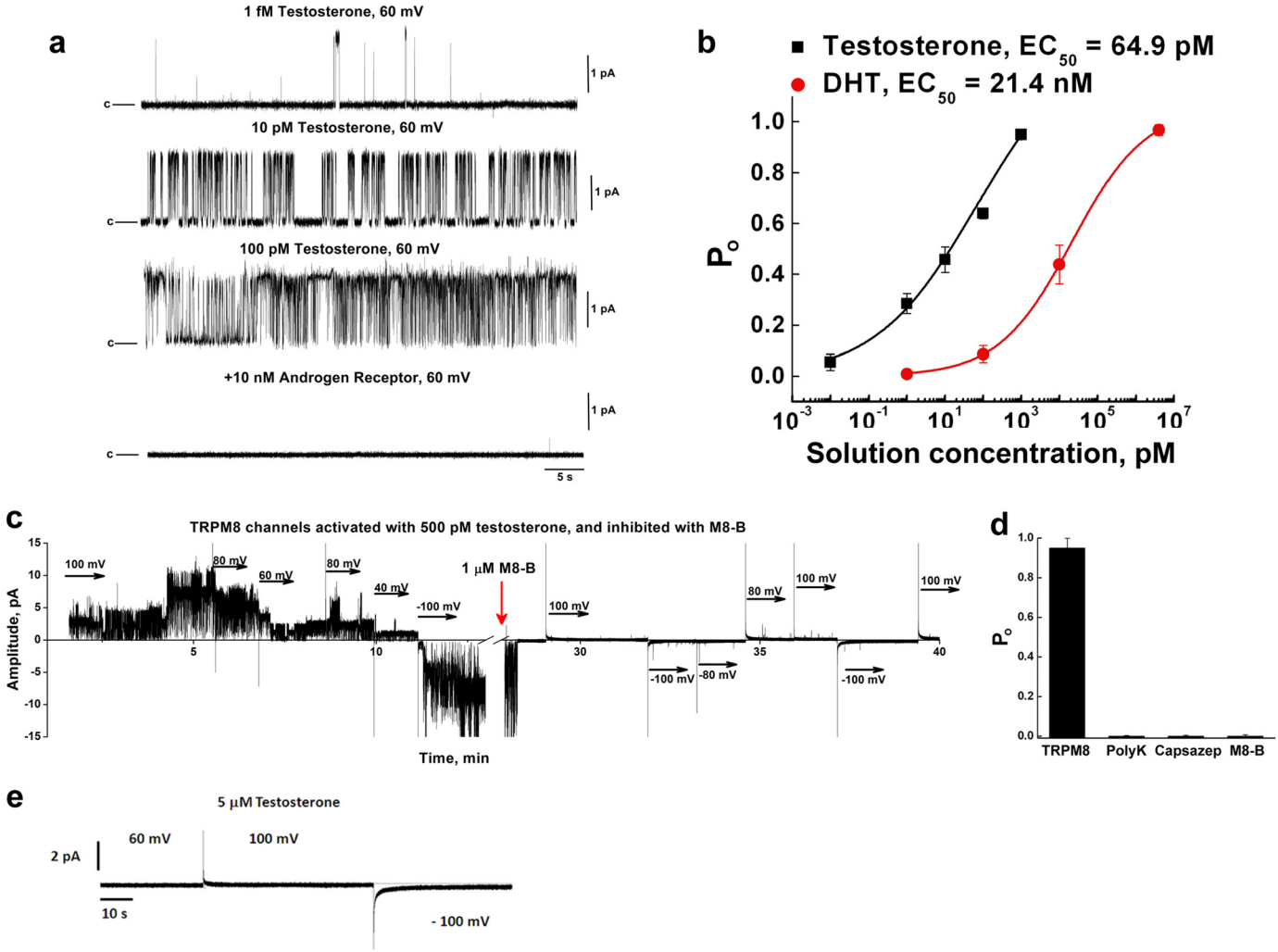

FIGURE 7. **Testosterone activates the TRPM8 channel in planar lipid bilayers.** *a*, TRPM8 channel openings induced by testosterone application. Representative single-channel current recordings of TRPM8 were obtained with different testosterone concentrations, as indicated *above* the current traces. The TRPM8 channel was incorporated in planar lipid bilayers formed from POPC/POPE (3:1) in *n*-decane between symmetric bathing solutions of 150 mM KCl, 0.2 mM $MgCl_2$, and 1 μM $CaCl_2$ in 20 mM HEPES buffer, pH 7.4, at 22 °C, in the presence of 2.5 μM DiC_8-PIP_2. The TRPM8 protein, at a concentration of 20 ng/ml, was incorporated into POPC/POPE micelles, which were added to the *cis* compartment (ground) with gentle stirring. The clamping potential was +60 mV. The *horizontal line* on the *left* of the traces and the letter *c* delineate the closed state of the channel. *b*, dose responses of testosterone and DHT as a function of the open probability of the TRPM8 channel obtained at +60 mV. Testosterone activation of TRPM8 has an EC_{50} of ~64.9 pM (n = 20), and DHT has an EC_{50} of ~21.4 nM (n = 9). *Error bars*, S.E. *c*, *d*, inhibition of testosterone-evoked TRPM8 channel activity with TRPM8 antagonists. *c*, representative current traces of TRPM8 channels activated with 500 pM testosterone and subsequently inhibited with 1 μM M8-B, a specific TRPM8 inhibitor. The addition of M8-B to only one side of the channel, presumably intracellular, did not inhibit the TRPM8 channel activity, whereas the addition to the other side, presumably extracellular, momentarily inhibited the channel openings. Before the addition of M8-B, TRPM8 channels were recorded for more than 2.5 h, where the channels were constantly gating. After the addition of M8-B, TRPM8 channels were inhibited for the rest of the recording (~2 h) and did not show any openings with different voltages. *d*, graph demonstrates inhibition of open probability for the TRPM8 channels activated with 500 pM testosterone and inhibited with 10 μg/ml polylysine (*polyK*) (n = 7), 10 μM capsazepine (n = 3), and 1 μM M8-B (n = 4) (*error bars*, S.E.). P_o values were obtained at 100 mV. *e*, control measurements were performed in the planar lipid bilayers in the absence of the TRPM8 protein. Conditions were the same as described in *a*. Testosterone concentrations were in the micromolar range (beginning from 1 μM and up to 5 μM), and the bilayers were challenged at various voltages for several h. No single event of channel-like behavior was observed. The control experiments were repeated four times.

required the presence of Ca^{2+} (Fig. 8*c*). On the contrary, the single channel mean slope conductance of testosterone-activated TRPM8, 37.1 ± 8.5 pS, was similar to the inward menthol-evoked mean slope conductance of 42.9 ± 1.6 pS (Fig. 8, *a* and *b*). These results indicate that the conductance and voltage-current relationship of TRPM8 are agonist-dependent.

An important hallmark of TRPM8 channel activity is requirement for PIP_2 (20, 21), and, as was shown previously, in planar lipid bilayers, TRPM8 cannot be activated with its common agonists in the absence of this phosphoinositide (11, 13). We found that the presence of PIP_2 is also required for TRPM8 activation with testosterone. Fig. 8*c* demonstrates that no channel activity can be detected with TRPM8 and testosterone alone; even when the channel was kept with the steroid for several h (n = 10), not a single channel-opening event was observed (Fig. 8*c*). The subsequent addition to the bilayers of 2.5 μM DiC_8-PIP_2 resulted in prompt channel opening (Fig. 8*c*). Testosterone-evoked single channel TRPM8 activity under non-saturated (10 pM) conditions demonstrated slight voltage dependence (Fig. 9).

Together, these results demonstrate that testosterone is a potent agonist that acts directly on the TRPM8 channel. Fur-

TABLE 1

LC MS/MS analysis demonstrating that TRPM8 is the major protein purified from HEK-293 cells stably expressing the channel

The peptide analysis was performed with the Mascot Search Engine, significance threshold $p < 0.05$, error range <10 ppm; the actual error range for the TRPM8 peptides was between ±0.01 and ±4.88 ppm. The TRPM8 protein was purified by immunoprecipitation with Myc antibodies.

Protein hits	Experiments	Protein Score	Number of Peptide Matches
TRPM8_RAT Transient receptor potential cation channel subfamily M member 8 OS=Rattus norvegicus	1 2 3	3364 3642 3354	149 147 207
TRYP_PIG Trypsin OS=Sus scrofa	1 2 3	414 411 579	25 22 44
K1C10_HUMAN Keratin, type I cytoskeletal 10 OS=Homo sapiens	1 2 3	389 410 521	17 15 39
K2C1_HUMAN Keratin, type II cytoskeletal 1 OS=Homo sapiens	1 2 3	375 410 564	17 15 29
G3P_HUMAN Glyceraldehyde-3-phosphate dehydrogenase OS=Homo sapiens	1 2 3	289 264 344	5 6 15
HS90B_HUMAN Heat shock protein HSP 90-beta OS=Homo sapiens	1 2 3	226 188 105	6 5 3
K1C14_HUMAN Keratin, type I cytoskeletal 14 OS=Homo sapiens	1 2 3	177 178 113	7 5 14
S10A6_MOUSE Protein S100-A6 OS=Mus musculus	1 2 3	135 160 94	4 4 4
K1C10_BOVIN Keratin, type I cytoskeletal 10 OS=Bos Taurus	1 2 3	128 -- 128	9 -- 3
K22E_HUMAN Keratin, type II cytoskeletal 2 epidermal OS=Homo sapiens	1 2 3	105 114 201	8 6 17
K1C9_HUMAN Keratin, type I cytoskeletal 9 OS=Homo sapiens	1 2 3	103 107 294	5 5 13
K2C5_BOVIN Keratin, type II cytoskeletal 5 OS=Bos Taurus	1 2 3	99 100 113	6 6 12
K1C17_HUMAN Keratin, type I cytoskeletal 17 OS=Homo sapiens	1 2 3	91 93 48	6 5 8
K1C19_HUMAN Keratin, type I cytoskeletal 19 OS=Homo sapiens	1 2 3	91 -- 48	5 -- 8
ADT1_HUMAN ADP/ATP translocase 1 OS=Homo sapiens	1 2 3	87 87 61	4 2 6
K2C5_HUMAN Keratin, type II cytoskeletal 5 OS=Homo sapiens	1 2 3	86 77 161	5 4 15

TABLE 1—*continued*

Protein hits	Experiments	Protein Score	Number of Peptide Matches
ACTN1_HUMAN	1	74	2
Alpha-actinin-1 OS=Homo sapiens	2	--	--
	3	--	--
MYH7_HUMAN	1	64	5
Myosin-7 OS=Homo sapiens	2	63	4
	3	173	18
TRY1_RAT	1	60	1
Anionic trypsin-1 OS=Rattus norvegicus	2	61	1
	3	84	8
TTC25_HUMAN	1	51	3
Tetratricopeptide repeat protein 25 OS=Homo sapiens	2	52	3
	3	28	4
S10AB_HUMAN	1	49	1
Protein S100-A11 OS=Homo sapiens	2	49	1
	3	118	3
ACTB_HUMAN	1	44	1
Actin, cytoplasmic 1 OS=Homo sapiens	2	40	1
	3	116	6
ACTA_HUMAN	1	39	2
Actin, aortic smooth muscle OS=Homo sapiens	2	38	1
	3	126	10
CNKR2_HUMAN	1	34	3
Connector enhancer of kinase suppressor of ras 2 OS=Homo sapiens	2	35	2
	3	30	3
RBM27_HUMAN	1	34	3
RNA-binding protein 27 OS=Homo sapiens	2	34	2
	3	--	--
KIF24_HUMAN	1	33	3
Kinesin-like protein KIF24 OS=Homo sapiens	2	30	2
	3	--	--
KDM5A_HUMAN	1	29	3
Lysine-specific demethylase 5A OS=Homo sapiens	2	25	2
	3	--	--
TNNC1_HUMAN	1	26	1
Troponin C, slow skeletal and cardiac muscles OS=Homo sapiens	2	--	--
	3	--	--
LAMA5_HUMAN	1	24	2
Laminin subunit alpha-5 OS=Homo sapiens	2	--	--
	3	--	--
NUDT6_HUMAN	1	22	3
Nucleoside diphosphate-linked moiety X motif 6 OS=Homo sapiens	2	--	--
	3	--	--

thermore, they confirm that TRPM8 activity is responsible for testosterone-induced ionotropic cellular responses.

Testosterone-binding Site to the TRPM8 Protein—In attempts to identify the specific testosterone-binding sites to TRPM8, we proceeded with the following strategy. The fast testosterone-induced responses with impermeant analog suggested that at least one of the steroid-interacting sites is located extracellularly (22). On the other hand, our recent findings demonstrated that extracellular post-translational modification of TRPM8 with polyester, PHB, is required for the channel activity with all of its known agonists (15). Considering that PHB may also be important for the interaction with testosterone on the extracellular side, we performed the IP assay with the PHB-deficient mutants. The WT TRPM8 and the PHB mutants, 5S-G and Y826G, were immunoprecipitated with DHT/testosterone antibodies and then probed with Myc antibodies. The amounts of the TRPM8 protein precipitated with testosterone decreased by ~40% for both PHB-deficient mutants (Fig. 10, *a* and *b*), further suggesting that this binding site may account for one of the interaction sites. Visualization of extracellular binding in immunocytochemistry experiments further showed strong testosterone interaction with the WT TRPM8 but not the PHB-deficient mutants (Fig. 10, *c* and *d*). These results indicate that extracellularly, testosterone might bind only to the PHB-modified channels (Fig. 10*e*). On the other hand, although PHB-deficient mutants significantly lack testosterone binding on the

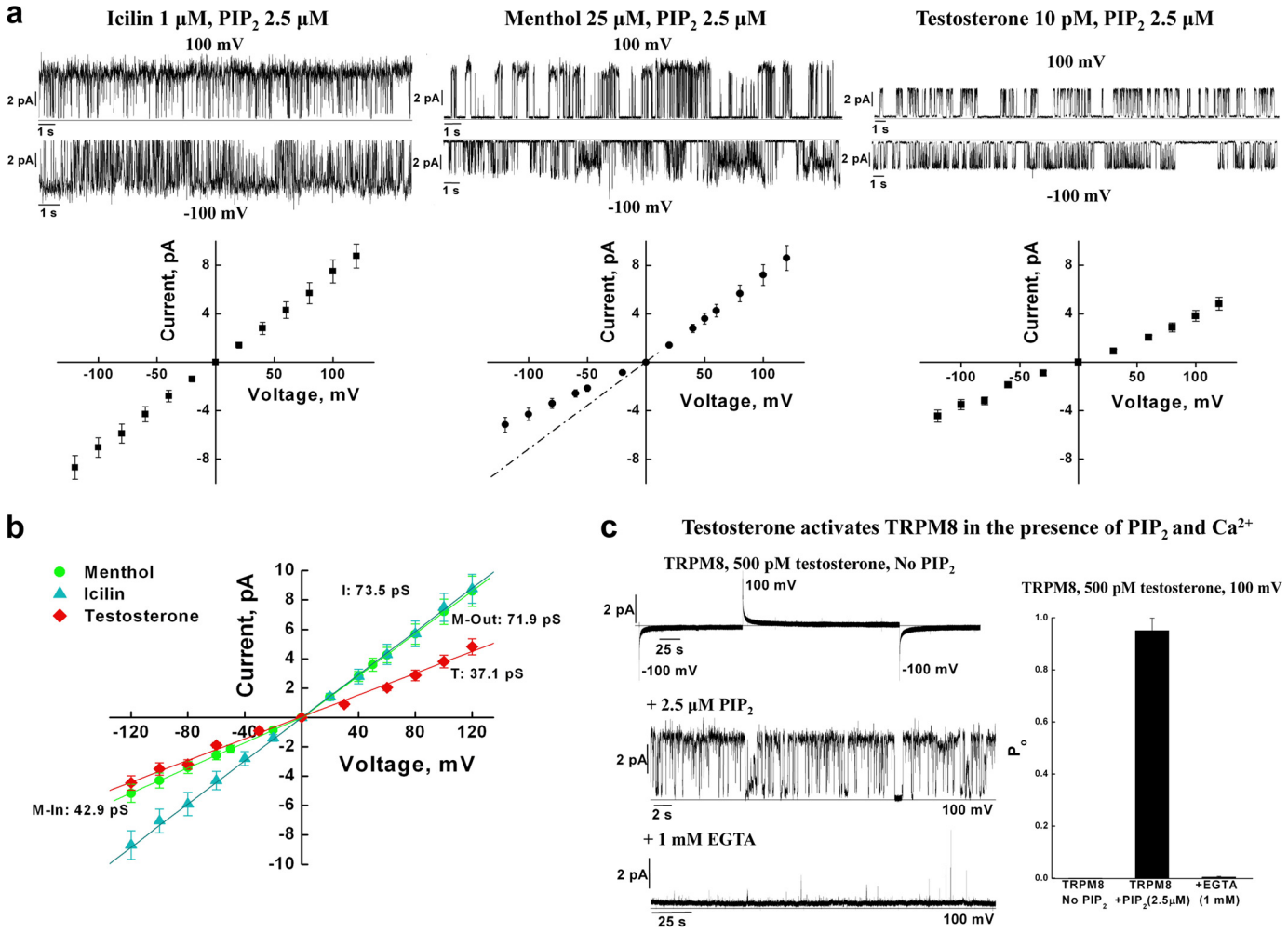

FIGURE 8. **Comparison of the TRPM8 single channel activity evoked by icilin, menthol, and testosterone in planar lipid bilayers.** *a*, representative single-channel current recordings and current-voltage relationship of TRPM8 obtained with icilin (1 μM), menthol (25 μM), and testosterone (10 pM). Experimental conditions are the same as described in the legend to Fig. 7; details are indicated on the *traces*. *b*, current (*I*)-voltage (*V*) relationship and mean slope conductance values of TRPM8 activated with icilin, menthol, and testosterone at the concentrations indicated in *a*, showing linear *I-V* curves for the icilin- and testosterone-evoked TRPM8 channels and the rectifying *I-V* curve for menthol-induced current. Mean slope single-channel conductance for icilin-activated TRPM8 is 73.5 $\pm$ 6.1 pS; menthol-activated outward conductance is 71.9 $\pm$ 3.5 pS; menthol-activated inward conductance is 42.9 $\pm$ 1.6 pS; testosterone-activated conductance is 37.1 $\pm$ 8.5 pS. *c*, testosterone activates TRPM8 in the presence of PIP_2 and Ca^{2+}. Representative current trace recordings demonstrate that no channel activity can be observed with TRPM8 and testosterone (500 pM) in planar lipid bilayers in the absence of PIP_2. The addition to the bilayers of 2.5 μM DiC_8-PIP_2 resulted in full opening of the channel ($n = 10$). The subsequent addition of 1 mM EGTA inhibits TRPM8 activity ($n = 4$). A summary is represented on the *right*.

extracellular side, reduction in testosterone binding to the whole protein is only partial (Fig. 10*b*). This suggests that other testosterone-interacting domains could be located internally, and those will have to be determined in the future.

To further test whether PHB-mediated testosterone binding to the TRPM8 protein is functionally important, we conducted Ca^{2+}-imaging experiments with the mutants. Both the 5S-G and Y826G mutants were insensitive to testosterone applications (Fig. 11).

Furthermore, to determine the possible testosterone-binding sites in TRPM8, we compared the protein sequences of TRPM8 and AR. These are very different proteins, and they do not share many similarities. Nonetheless, TRPM8 and AR sequence alignment revealed interesting details. Only three peptides showed some relative resemblance between these two proteins, and, surprisingly, two of these peptides from AR belong to the androgen-binding domain, according to the crystal structure of the protein (23), and one peptide from TRPM8 is located in the functionally critical region of the extracellular PHB-binding domain (15). Although the sequence similarity is of low percentage, the critical residues Tyr-826 and Ser-827 in the PHB-binding peptide of TRPM8 are conserved in the corresponding peptide from the AR protein (Fig. 12).

Acute Testosterone Application on Skin Elicits a Cooling Sensation—Thus far, our experiments indicated that testosterone is an endogenous agonist of the TRPM8 channel. This finding raises an important question. Does acute testosterone application on the skin surface elicit a cooling sensation? Single-blinded tests were performed by applying various doses of testosterone to skin, and the durations of the responses were recorded. Ethanol and menthol applications were used as controls. We found that acute testosterone application on the skin did elicit a cooling sensation, and its duration differed by gender (Fig. 13). The female volunteers experienced a cooling sensation for a longer duration, and at higher con-

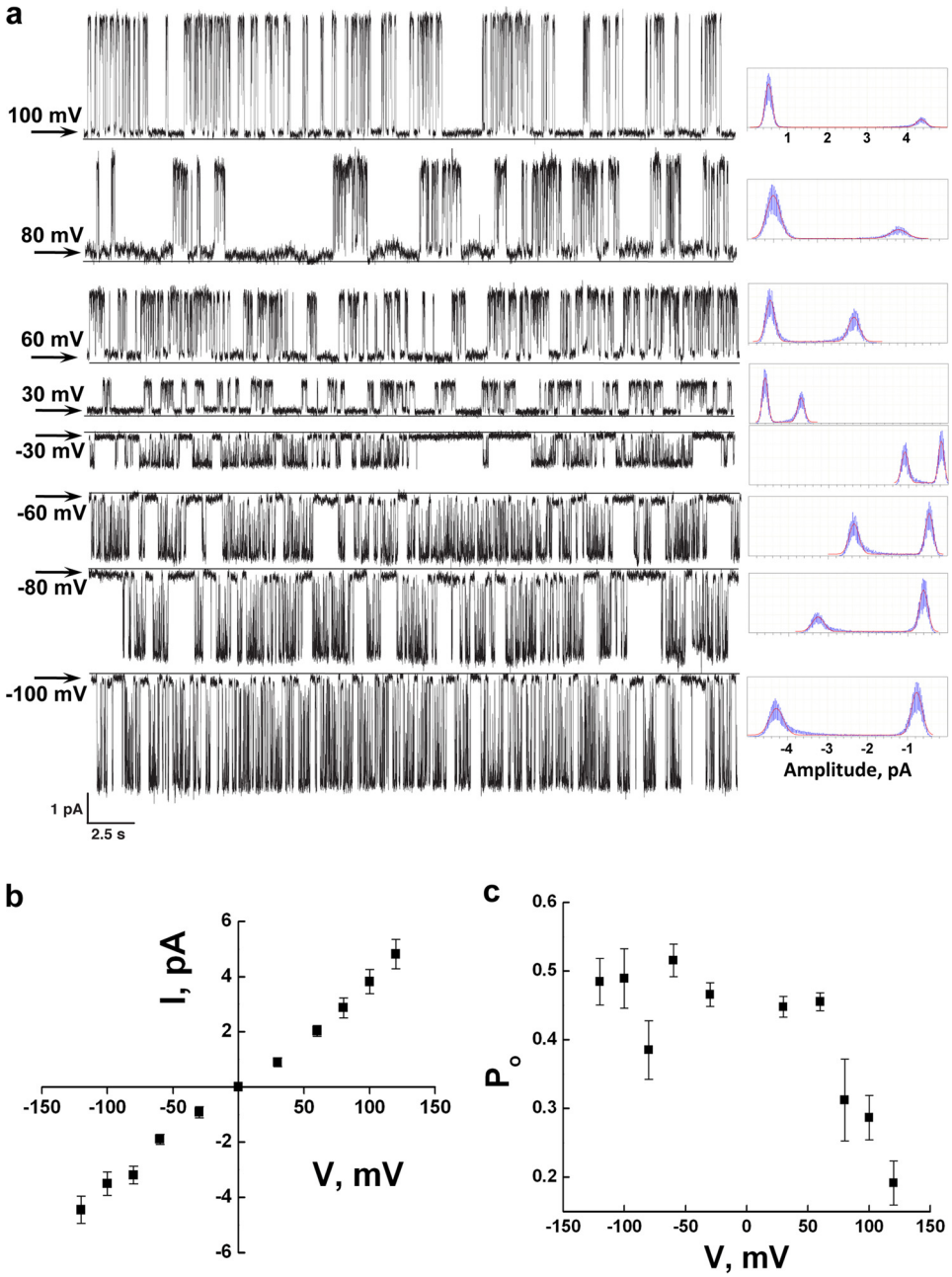

FIGURE 9. **Single channel activity of TRPM8 obtained under non-saturated conditions, activated with 10 pM testosterone, in planar lipid bilayers.** *a*, representative current traces and all-points histograms of TRPM8 activated with 10 pM testosterone obtained at different voltages, as indicated on the *traces*. The experimental conditions are the same as indicated in the legend to Fig. 7*a*. Shown are the current-voltage relationship (*b*) and shows open probability values (*c*) of TRPM8 activated with 10 pM testosterone obtained at different voltages.

centrations of testosterone, the sensation further developed into a slight pain sensation, which was described as slight stinging or pinching effects (Fig. 13). Unlike the females, the male volunteers experienced shorter cooling effects that rarely developed into a pain sensation (Fig. 13). These results indicate that TRPM8 channels are more desensitized in males, who have higher levels of testosterone, whereas TRPM8 is more readily activated in females, who have naturally lower levels of testosterone.

The complex regulation of testosterone-induced TRPM8 activity, including its competitive binding to the AR protein that further introduces an inhibitory mechanism, is depicted in the schematic representation in Fig. 14.

DISCUSSION

Testosterone, a steroid hormone from the androgen family, is largely known for its classic genomic actions, with the steroid binding to the nuclear androgen receptor and the subsequent regulation of gene expression (24). However, androgens may also exert rapid non-genomic actions that have long been evidenced in different cellular systems (4, 25). These actions do not involve the classic androgen receptor pathway but, rather, suggest the participation of a signal-generating membrane surface receptor. In particular, rapid testosterone-induced intracellular Ca^{2+} elevations have been observed in a variety of cell types, including rat Sertoli cells, human prostatic cells

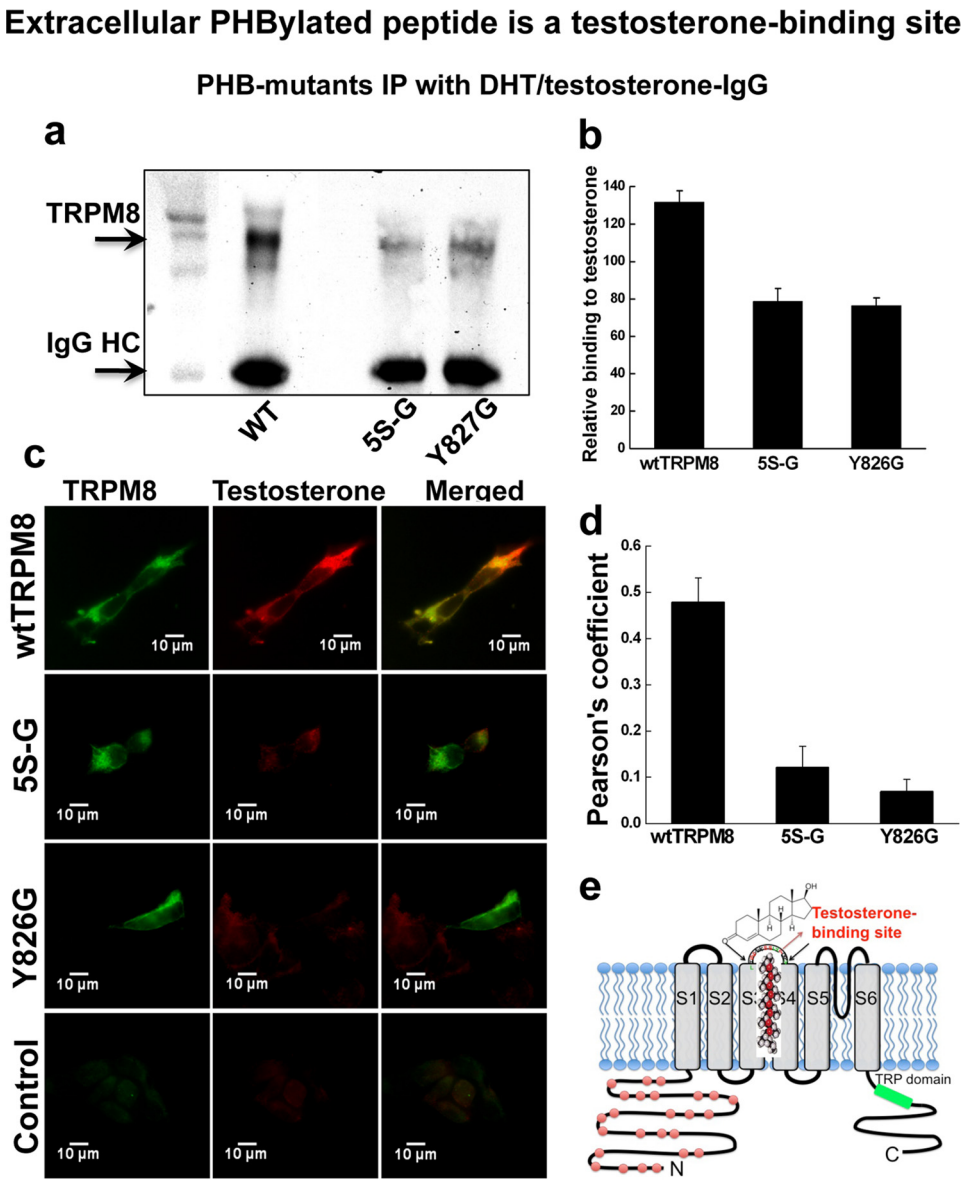

FIGURE 10. **Extracellular PHBylated peptide is one of the testosterone-binding sites.** *a*, IP performed with the WT TRPM8 and PHB mutants, 5S-G and Y826G. *b*, summary of the relative binding to testosterone for the WT TRPM8 and PHB mutants. *c, d,* PHB mutants of TRPM8 show a dramatic decrease in the channel colocalization with testosterone on plasma membrane. *c*, immunocytochemistry was done with the HEK-293 cells transiently expressing WT TRPM8 and PHB mutants 5S-G and Y826G. After fixing with 2% paraformaldehyde for 30 min and BSA blocking, nonpermeabilized cells were treated with 1 nM testosterone for 1 h following incubation with anti-Myc-IgG for the protein and anti-DHT/testosterone-IgG for testosterone detection. Cell images were obtained with Olympus BX61 confocal microscope and were analyzed with ImageJ software. *d*, the Pearson coefficients for colocalization of testosterone with the WT TRPM8 protein or PHB mutants were calculated using the Colocalization Finder plugin of the ImageJ software. *e*, model of the TRPM8 protein demonstrates testosterone binding to PHBylated peptide on the extracellular side.

(LNCaP and PC3) (22), rat heart myocytes (26), male (but not female) rat osteoblasts (27), and mouse T cells lacking the functional AR protein (28, 29). However, the molecular identity of the hypothesized membrane testosterone receptor remained unknown.

While attempting to identify an ionotropic testosterone receptor, we serendipitously discovered its affinity for the TRPM8 protein. The role of this cold and menthol receptor is well understood in the framework of the somatosensory system, and appreciation of TRPM8 in the perception of the surrounding environment and pain stimuli is nowadays widely applicable in therapeutics. However, historically, the TRPM8 protein was first found in the prostate glandular cells, due to its high expression levels (7), but its role in the prostate has remained elusive since its discovery. Indeed, despite a large body of literature addressing the expression and function of TRPM8 in the prostate (30–35), uncertainty remained regarding the role of this channel in the prostate gland, mainly because no natural agonists that endogenously activate TRPM8 had been identified. Our discovery that TRPM8 acts as a membrane testosterone receptor sheds light on processes in every cell type/tissue where it is discovered, including sensory modulation, temper, and behavioral changes. Because TRPM8 channels have relatively high selectivity for Ca^{2+} and little selectivity among monovalent cations (8), testosterone-induced ionotropic actions medi-

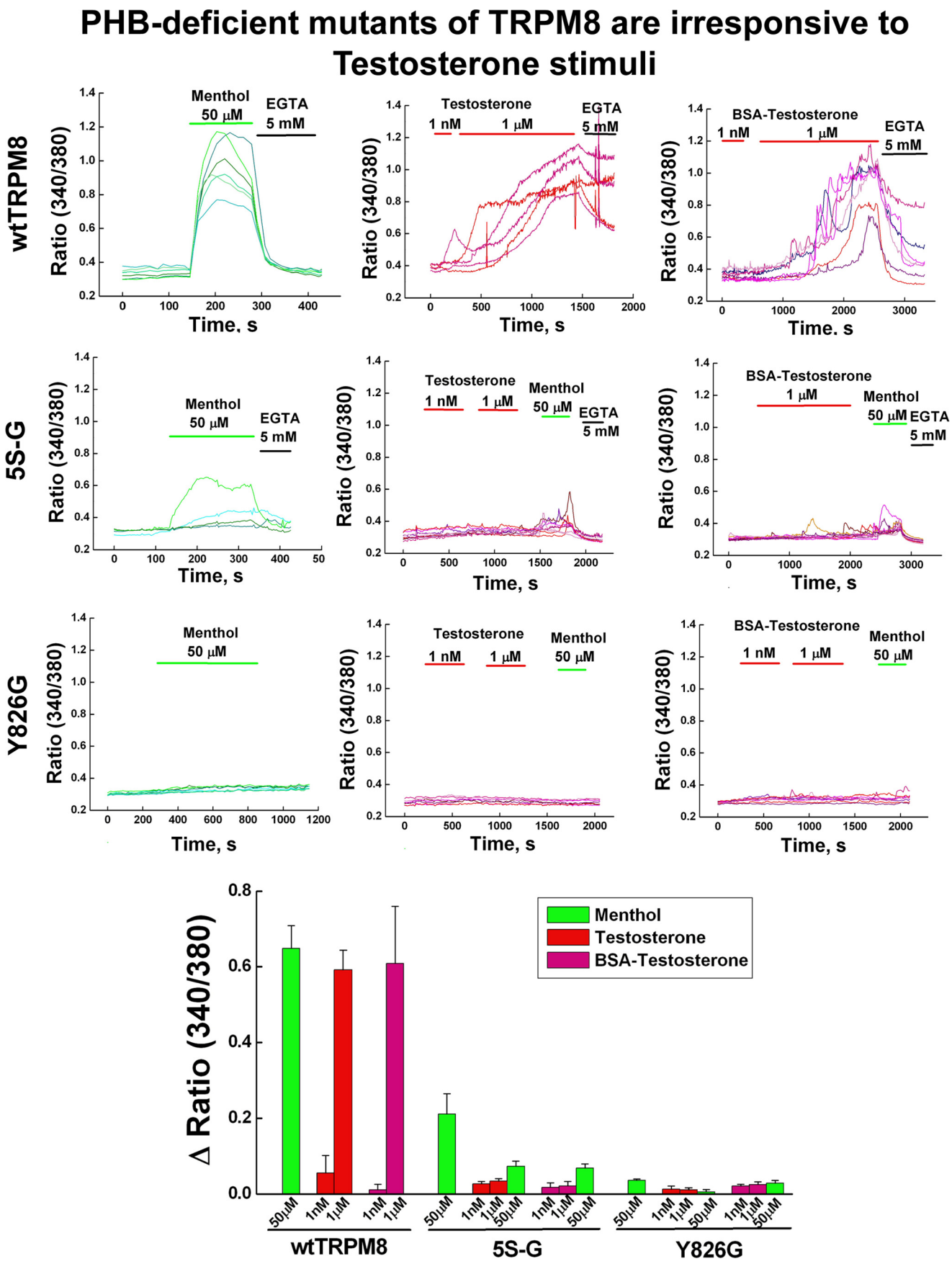
PHB-deficient mutants of TRPM8 are irresponsive to Testosterone stimuli
wtTRPM8
5S-G
Y826G
Ratio (340/380)
Time, s
Menthol
50 μM
EGTA
5 mM
Testosterone
1 nM
1 μM
BSA-Testosterone
Δ Ratio (340/380)
wtTRPM8
5S-G
Y826G

Alignment statistics for match #1

Score	Expect	Method	Identities	Positives	Gaps
20.8 bits(42)	0.45	Compositional matrix adjust.	11/30(37%)	14/30(46%)	0/30(0%)

```
TRPM8   18   LDSTRTLYSSASRSTDLSYSESDLVNFIQA   47    PHB-binding(internal
             L ST +LY S +      +Y   D  NF  A
AR     339   LPSTLSLYKSGALDEAAAYQSRDYYNFPLA   368
```

Alignment statistics for match #2

Score	Expect	Method	Identities	Positives	Gaps
20.8 bits(42)	0.46	Compositional matrix adjust.	8/22(36%)	13/22(59%)	0/22(0%)

```
TRPM8   806   LFYFIAGIVFRLHSSNKSSLYS   827    PHB-binding(external)
              + YF   +VF  +  +KS +YS
AR      761   MLYFAPDLVFNEYRMHKSRMYS   782    Androgen-binding domain
```

Alignment statistics for match #3

Score	Expect	Method	Identities	Positives	Gaps
16.9 bits(32)	8.4	Compositional matrix adjust.	4/14(29%)	8/14(57%)	0/14(0%)

```
TRPM8   619   NEYETRAVELFTEC   632
              NEY      ++++C
AR      771   NEYRMHKSRMYSQC   784    Androgen-binding domain
```

FIGURE 12. **Bioinformatics analysis of the TRPM8 and the AR proteins.** The protein sequence alignment for TRPM8 and AR reveals three peptides that share some similarity. Interestingly, two of the peptides from the AR protein belong to the androgen-binding domain, and two peptides of TRPM8 are modified by PHB, including intracellular and extracellular modifications (15).

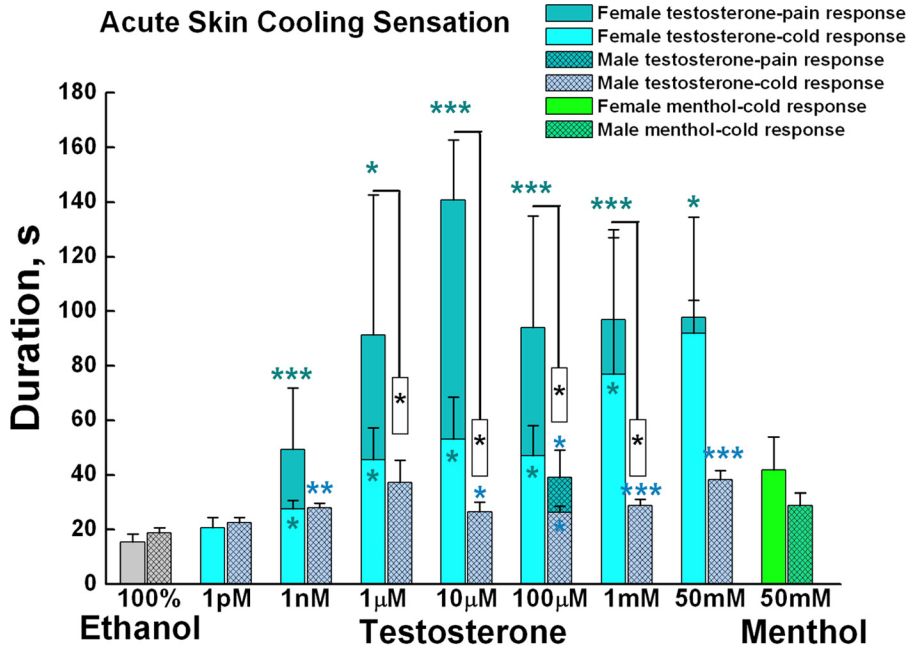

FIGURE 13. **Testosterone elicits a cooling sensation upon acute topical skin application.** Sixteen healthy volunteers (eight female and eight male) between the ages of 18 and 55 years were recruited for the single-blind test. Testosterone was applied in different concentrations and orders on the skin surface, and the durations of the responses were recorded. The volunteers described their sensation as a feeling of cold and, for the higher agonist concentrations, as mixed feelings of cold and stinging. The duration of the cold-evoked responses was significantly longer in the female volunteers than in the males at the following concentrations of testosterone: 1 pM, $p = 0.928$; 1 nM, $p = 0.559$; 1 μM, $p = 0.190$; 10 μM, $p = 0.031$ (*); 100 μM, $p = 0.039$ (*); 1 mM, $p = 0.014$ (*); 50 mM, $p = 0.136$; for 50 mM menthol, $p = 0.324$. Females demonstrated significant difference in the cold duration compared with ethanol: 1 pM, $p = 0.282$; 1 nM cold response, $p = 0.015$ (*); 1 nM pain response, $p = 0.0036$ (***); 1 μM cold response, $p = 0.024$ (*); 1 μM pain response, $p = 0.016$ (*); 10 μM cold response, $p = 0.033$ (*); 10 μM pain response, $p = 0.002$ (***); 100 μM cold response, $p = 0.015$ (*); 100 μM pain response, $p = 0.0019$ (***); 1 mM cold response, $p = 0.0139$ (*); 1 mM pain response, $p = 3.4E-5$ (***); 50 mM cold response, $p = 0.1001$; 50 mM pain response, $p = 0.027$ (*); 50 mM menthol/cold response, $p = 0.050$. Males demonstrated significant difference in the cold duration compared with ethanol: 1 pM, $p = 0.124$; 1 nM cold response, $p = 0.0027$ (**); 1 μM cold response, $p = 0.054$; 10 μM cold response, $p = 0.048$ (*); 100 μM cold response, $p = 0.021$ (*); 100 μM pain response, $p = 0.0126$ (*); 1 mM cold response, $p = 0.004$ (***); 50 mM cold response, $p = 0.0003$ (***); 50 mM menthol/cold response, $p = 0.065$. The graph shows *dark cyan asterisks* for statistical difference between female cold/pain responses and female ethanol responses and *blue asterisks* for statistical difference between male cold/pain responses and male ethanol responses; *black asterisks* show significant difference between two genders. *Error bars*, S.E.

ated by TRPM8 may be important regulators of the cell cycle through Ca^{2+} homeostasis.

The high level of colocalization observed in samples of human prostate tissues shows that TRPM8 and testosterone are probably interacting, whether on the plasma membrane of the prostate periphery or on the ER membranes in the lumen cells (19). The IP experiments further confirmed direct molecular interaction between TRPM8 and testosterone (19). Subse-

FIGURE 11. **PHB-deficient mutants of TRPM8 are irresponsive to testosterone stimuli.** Fluorescence measurements of intracellular Ca^{2+} concentration were performed on WT TRPM8 and PHB mutants, 5S-G and Y826G, transiently expressed in HEK-293 cells cultured under the steroid-deprived conditions. *Bottom*, summary graph. Error bars, S.E.

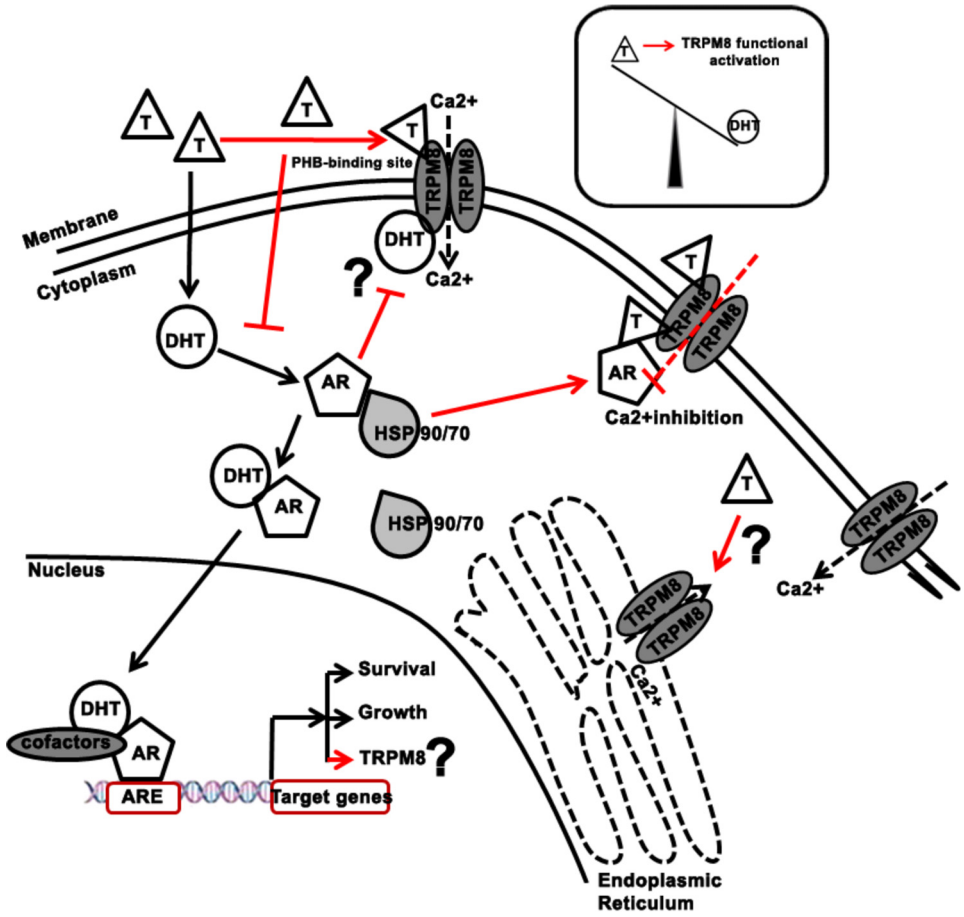

FIGURE 14. **Schematic representation of testosterone-induced TRPM8 channel activity.** The scheme represents TRPM8 as an ionotropic testosterone receptor, which has higher affinity for testosterone than for DHT. The figure also depicts the genomic androgen-dependent regulation of TRPM8 expression.

quently, the Ca^{2+}-imaging experiments on PC3, DRG neurons, and hippocampal neurons revealed that testosterone is a potent agonist of the TRPM8 channel (Figs. 1 and 2). Given that testosterone might be involved in several regulatory pathways, including inositol 1,4,5-triphosphate signaling (17) and G-protein coupled receptor (GPCR6A) regulation (16), the best evidence we provide in this work is direct activation of TRPM8 with testosterone in planar lipid bilayers (Figs. 7–9).

Steroid regulation of transient receptor potential channels is not uncommon. It has recently been shown that another melastatin subfamily member, TRPM3, is an ionotropic steroid receptor that can be activated by pregnenolone sulfate, a neuroactive steroid (36). However, unlike TRPM8, which is activated by testosterone in the picomolar range (Figs. 1, 2, and 7–9), TRPM3 is activated by pregnenolone sulfate with micromolar concentrations. This difference indicates that TRPM8 is a highly selective, sensitive, and potent testosterone receptor. Moreover, testosterone activates TRPM8 with a higher potency (EC_{50} ~65 pM) than DHT (EC_{50} ~21 nM) (Fig. 7*b*). It is noteworthy that testosterone's affinity for the classic androgen receptor protein falls in a similar concentration range (K_d ~70 pM) (37). This indicates that testosterone's affinity to TRPM8 is comparable with that of the AR protein and suggests similar specificity. Furthermore, the picomolar concentrations of testosterone that are sufficient to activate TRPM8 channels are in agreement with the rapid androgen actions observed in different cell systems (22). Consideration of increased fluidity of the membrane with testosterone application is unlikely, because, in comparison with other steroids, even at high concentration, testosterone has little effect on membrane fluidity, aggregation, and leakage (4).

The conductance values and current-voltage relationship of TRPM8 activated with testosterone differed from those when the channel is activated by menthol or icilin. Interestingly, the conductance values were similar to the menthol-activated inward conductance (see Fig. 8*b*, negative voltages); however, in the case of testosterone, the overall current-voltage relationship was linear, similar to that when the channel is activated with icilin (Fig. 8*b*) and unlike menthol activation, which demonstrates inward rectification (Fig. 8, *a* and *b*). This indicates that these properties of TRPM8 are agonist-specific. The differences might be explained by the possibility that TRPM8 channel can adopt distinct conformation states when allosterically regulated by its agonists. Interestingly, recent advances in the electron cryomicroscopy made it possible to obtain the structural information of TRPV1. The TRPV1 structure was resolved at high resolution and provided important insights into the molecular arrangements of the channel alone or in complex with its ligands (12). In this work, the authors demonstrated that in the presence of different agonists, the TRPV1 channel pore region acquires discernible conformations and

various diameters of the permeation path (12). It is possible that similar conformational changes might take place in TRPM8.

As for the current-voltage relationship, which is attributed to the voltage-dependence of TRPM8 and its signature outward rectification, it should be noted that testosterone binds to more than one binding site, which may affect the voltage sensitivity of the channel. In line with this finding, lack of the outward rectification was also observed for icilin-induced TRPM8 currents in patch clamp recordings (21) as well as in planar lipid bilayers (13).

The activation of TRPM8 with an impermeable testosterone covalently conjugated to BSA (Figs. 1, 3, and 4) is also in line with the previous reports on intracellular Ca^{2+} fluxes observed with this analog in different cellular systems (22, 27, 29). This indicates that at least one of the testosterone-interacting sites is located on the extracellular side of the channel. On the other hand, our recent findings show that the PHB modification that is required for the TRPM8 channel function is also localized extracellularly (15). We tested whether the extracellular PHBylated peptides of TRPM8 are involved in the interactions with testosterone. Indeed, IP and immunocytochemistry experiments demonstrated a significant reduction of testosterone/TRPM8 binding in the PHB-deficient mutants, which were also testosterone-insensitive (Figs. 10 and 11). This finding further enhances the role of PHB modification in TRPM8 channels, where the polymer not only contributes to the conformational changes of the protein but also serves as a ligand-binding acceptor.

Additionally, acute applications of testosterone on the skin surface elicited a cooling sensation in female and male volunteers (Fig. 13). Interestingly, the female volunteers experienced a cooling sensation for a longer duration than the males, indicating that TRPM8 channels are more desensitized in males, who naturally have higher testosterone levels. At the same time, TRPM8 was more readily activated in females, who have naturally lower levels of testosterone. These results may also explain why females in general are more susceptible to cold temperatures than males.

Overall, our data strongly suggest a novel role for the TRPM8 ion channel as a testosterone receptor (Fig. 14). These results indicate the importance of TRPM8 in a wide range of physiological processes that involve the steroid hormone testosterone, including processes in the central nervous and male reproductive systems.

Acknowledgments—We thank Dr. Harel Weinstein for reading the manuscript and providing insightful recommendations. We also are very thankful to Dr. Natalia Shirokova for reading the manuscript and providing valuable comments. We are grateful for the insightful review and valuable recommendations received from Dr. Elizabeth A. Jonas. We thank Dr. Valerie Chappe for use of the patch clamp setup.

REFERENCES

1. Beato, M., Chávez, S., and Truss, M. (1996) Transcriptional regulation by steroid hormones. *Steroids* **61,** 240–251
2. Bruck, N., Bastien, J., Bour, G., Tarrade, A., Plassat, J. L., Bauer, A., Adam-Stitah, S., and Rochette-Egly, C. (2005) Phosphorylation of the retinoid X receptor at the ω loop modulates the expression of retinoic-acid-target genes with a promoter context specificity. *Cell. Signal.* **17,** 1229–1239
3. Wierman, M. E. (2007) Sex steroid effects at target tissues: mechanisms of action. *Adv. Physiol. Educ.* **31,** 26–33
4. Wehling, M. (1997) Specific, nongenomic actions of steroid hormones. *Annu. Rev. Physiol.* **59,** 365–393
5. Jones, R. D., Pugh, P. J., Jones, T. H., and Channer, K. S. (2003) The vasodilatory action of testosterone: a potassium-channel opening or a calcium antagonistic action? *Br. J. Pharmacol.* **138,** 733–744
6. Sabnis, A. S., Shadid, M., Yost, G. S., and Reilly, C. A. (2008) Human lung epithelial cells express a functional cold-sensing TRPM8 variant. *Am. J. Respir. Cell Mol. Biol.* **39,** 466–474
7. Tsavaler, L., Shapero, M. H., Morkowski, S., and Laus, R. (2001) Trp-p8, a novel prostate-specific gene, is up-regulated in prostate cancer and other malignancies and shares high homology with transient receptor potential calcium channel proteins. *Cancer Res.* **61,** 3760–3769
8. McKemy, D. D., Neuhausser, W. M., and Julius, D. (2002) Identification of a cold receptor reveals a general role for TRP channels in thermosensation. *Nature* **416,** 52–58
9. Peier, A. M., Moqrich, A., Hergarden, A. C., Reeve, A. J., Andersson, D. A., Story, G. M., Earley, T. J., Dragoni, I., McIntyre, P., Bevan, S., and Patapoutian, A. (2002) A TRP channel that senses cold stimuli and menthol. *Cell* **108,** 705–715
10. Bautista, D. M., Siemens, J., Glazer, J. M., Tsuruda, P. R., Basbaum, A. I., Stucky, C. L., Jordt, S.-E., and Julius, D. (2007) The menthol receptor TRPM8 is the principal detector of environmental cold. *Nature* **448,** 204–208
11. Zakharian, E., Thyagarajan, B., French, R. J., Pavlov, E., and Rohacs, T. (2009) Inorganic polyphosphate modulates TRPM8 channels. *PLoS One* **4,** e5404
12. Cao, E., Liao, M., Cheng, Y., and Julius, D. (2013) TRPV1 structures in distinct conformations reveal activation mechanisms. *Nature* **504,** 113–118
13. Zakharian, E., Cao, C., and Rohacs, T. (2010) Gating of transient receptor potential melastatin 8 (TRPM8) channels activated by cold and chemical agonists in planar lipid bilayers. *J. Neurosci.* **30,** 12526–12534
14. Zakharian, E. (2013) Recording of ion channel activity in planar lipid bilayer experiments. *Methods Mol. Biol.* **998,** 109–118
15. Cao, C., Yudin, Y., Bikard, Y., Chen, W., Liu, T., Li, H., Jendrossek, D., Cohen, A., Pavlov, E., Rohacs, T., and Zakharian, E. (2013) Polyester modification of the mammalian TRPM8 channel protein: implications for structure and function. *Cell Rep.* **4,** 302–315
16. Pi, M., Parrill, A. L., and Quarles, L. D. (2010) GPRC6A mediates the non-genomic effects of steroids. *J. Biol. Chem.* **285,** 39953–39964
17. Estrada, M., Liberona, J. L., Miranda, M., and Jaimovich, E. (2000) Aldosterone- and testosterone-mediated intracellular calcium response in skeletal muscle cell cultures. *Am. J. Physiol. Endocrinol. Metab.* **279,** E132–E139
18. Almeida, M. C., Hew-Butler, T., Soriano, R. N., Rao, S., Wang, W., Wang, J., Tamayo, N., Oliveira, D. L., Nucci, T. B., Aryal, P., Garami, A., Bautista, D., Gavva, N. R., and Romanovsky, A. A. (2012) Pharmacological blockade of the cold receptor TRPM8 attenuates autonomic and behavioral cold defenses and decreases deep body temperature. *J. Neurosci.* **32,** 2086–2099
19. Asuthkar, S., Elustondo, P. A., Demirkhanyan, L., Sun, X., Baskaran, P., Velpula, K. K., Thyagarajan, B., Pavlov, E. V., and Zakharian, E. (2015) The TRPM8 protein is a testosterone receptor. I. Biochemical evidence for direct TRPM8-testosterone interactions. *J Biol. Chem.* **290,** 2659–2669
20. Liu, B., and Qin, F. (2005) Functional control of cold- and menthol-sensitive TRPM8 ion channels by phosphatidylinositol 4,5-bisphosphate. *J. Neurosci.* **25,** 1674–1681
21. Rohács, T., Lopes, C. M., Michailidis, I., and Logothetis, D. E. (2005) PI(4,5)P2 regulates the activation and desensitization of TRPM8 channels through the TRP domain. *Nat. Neurosci.* **8,** 626–634
22. Lyng, F. M., Jones, G. R., and Rommerts, F. F. (2000) Rapid androgen actions on calcium signaling in rat sertoli cells and two human prostatic cell lines: similar biphasic responses between 1 picomolar and 100 nanomolar concentrations. *Biol. Reprod.* **63,** 736–747
23. Sack, J. S., Kish, K. F., Wang, C., Attar, R. M., Kiefer, S. E., An, Y., Wu, G. Y.,

Scheffler, J. E., Salvati, M. E., Krystek, S. R., Jr., Weinmann, R., and Einspahr, H. M. (2001) Crystallographic structures of the ligand-binding domains of the androgen receptor and its T877A mutant complexed with the natural agonist dihydrotestosterone. *Proc. Natl. Acad. Sci. U.S.A.* **98,** 4904–4909

24. Beato, M., and Sánchez-Pacheco, A. (1996) Interaction of steroid hormone receptors with the transcription initiation complex. *Endocr. Rev.* **17,** 587–609
25. Revelli, A., Massobrio, M., and Tesarik, J. (1998) Nongenomic actions of steroid hormones in reproductive tissues. *Endocr. Rev.* **19,** 3–17
26. Koenig, H., Fan, C. C., Goldstone, A. D., Lu, C. Y., and Trout, J. J. (1989) Polyamines mediate androgenic stimulation of calcium fluxes and membrane transport in rat heart myocytes. *Circ. Res.* **64,** 415–426
27. Lieberherr, M., and Grosse, B. (1994) Androgens increase intracellular calcium concentration and inositol 1,4,5-trisphosphate and diacylglycerol formation via a pertussis toxin-sensitive G-protein. *J. Biol. Chem.* **269,** 7217–7223
28. Benten, W. P., Lieberherr, M., Sekeris, C. E., and Wunderlich, F. (1997) Testosterone induces Ca^{2+} influx via non-genomic surface receptors in activated T cells. *FEBS Lett.* **407,** 211–214
29. Benten, W. P., Lieberherr, M., Giese, G., Wrehlke, C., Stamm, O., Sekeris, C. E., Mossmann, H., and Wunderlich, F. (1999) Functional testosterone receptors in plasma membranes of T cells. *FASEB J.* **13,** 123–133
30. Bidaux, G., Flourakis, M., Thebault, S., Zholos, A., Beck, B., Gkika, D., Roudbaraki, M., Bonnal, J.-L., Mauroy, B., Shuba, Y., Skryma, R., and Prevarskaya, N. (2007) Prostate cell differentiation status determines transient receptor potential melastatin member 8 channel subcellular localization and function. *J. Clin. Invest.* **117,** 1647–1657
31. Bidaux, G., Roudbaraki, M., Merle, C., Crépin, A., Delcourt, P., Slomianny, C., Thebault, S., Bonnal, J. L., Benahmed, M., Cabon, F., Mauroy, B., and Prevarskaya, N. (2005) Evidence for specific TRPM8 expression in human prostate secretory epithelial cells: functional androgen receptor requirement. *Endocr. Relat. Cancer* **12,** 367–382
32. Gkika, D., Flourakis, M., Lemonnier, L., and Prevarskaya, N. (2010) PSA reduces prostate cancer cell motility by stimulating TRPM8 activity and plasma membrane expression. *Oncogene* **29,** 4611–4616
33. Thebault, S., Lemonnier, L., Bidaux, G., Flourakis, M., Bavencoffe, A., Gordienko, D., Roudbaraki, M., Delcourt, P., Panchin, Y., Shuba, Y., Skryma, R., and Prevarskaya, N. (2005) Novel role of cold/menthol-sensitive transient receptor potential melastatine family member 8 (TRPM8) in the activation of store-operated channels in LNCaP human prostate cancer epithelial cells. *J. Biol. Chem.* **280,** 39423–39435
34. Zhang, L., and Barritt, G. J. (2004) Evidence that TRPM8 is an androgen-dependent Ca^{2+} channel required for the survival of prostate cancer cells. *Cancer Res.* **64,** 8365–8373
35. Bandell, M., Dubin, A. E., Petrus, M. J., Orth, A., Mathur, J., Hwang, S. W., and Patapoutian, A. (2006) High-throughput random mutagenesis screen reveals TRPM8 residues specifically required for activation by menthol. *Nat. Neurosci.* **9,** 493–500
36. Wagner, T. F., Loch, S., Lambert, S., Straub, I., Mannebach, S., Mathar, I., Düfer, M., Lis, A., Flockerzi, V., Philipp, S. E., and Oberwinkler, J. (2008) Transient receptor potential M3 channels are ionotropic steroid receptors in pancreatic beta cells. *Nat. Cell Biol.* **10,** 1421–1430
37. Michel, G., and Baulieu, E. E. (1980) Androgen receptor in rat skeletal muscle: characterization and physiological variations. *Endocrinology* **107,** 2088–2098